INSULATION DEGRADATION UNDER FAST, REPETITIVE VOLTAGE PULSES

WG D1.43

Members

A. Cavallini, **Convenor** (IT), D. Fabiani, **Secretary** (IT),

Hatano Hiroshi (JP), Nagao Masayuki (JP), Holboell Joachim (DK), Lee June-Ho (KR), Stone Greg (CA), Sedding Howard (CA), Doyle John (IE), Cancado Álvaro Batista (BR), Espino Fermin (MX), Claudi Albert (DE), Dong-Jin Park (KR), Hiroyuki Yamashita (JP)

ISBN : (To be completed by CIGRE)

ISBN : (To be completed by CIGRE)

Insulation degradation under fast, repetitive voltage pulses

TYPE SUBTITLE IF APPLICABLE

No Extra Cover page or "blank pages"
Use CIGRE abbreviations insofar as possible:Study Committee – SC, Technical Brochure – TB, Working Group – WG
Joint Working Group – JWG, Technical Committee – TC
Photos: must be of reasonable definition (preferably 300 dpi); all figures and tables must be titled, legible and numbered with legends provided.
No Company logos…

Table of Contents

EXECUTIVE SUMMARY

The use of power electronics in industrial drives has brought several advantages (e.g. flexibility of electrical energy conversion including regenerative bracking, more compact and lightweight drives). However, the use of power converters has been associated, already at the end of the eighties of the last century, with the reduced reliability of several components (the stators of low voltage random wound motors have experienced the most dramatic loss of reliability). In the future, these effects will become more and more an issue in the future due to the ubiquitous use of power converters in smart grids.

This brochure is aimed at presenting, for a number of equipment typologies, the reasons behind accelerated degradation of insulation systems subjected to repetitive surges induced by power electronic converters. Also, the solutions provided by the International Electrotechnical Commission for induction motors will be discussed, as they might for a reference for other type of electrical components. Eventually, the use of nanodielectrics as a tool to alleviate the aforementioned problems will be discussed.

LISTS

List of abbreviations

- EUT: Equipment Under Test
- HVDC: High Voltage Direct Current
- IRV: Impulse Rated Voltage
- PD: Partial Discharge
- PDIV: Partial Discharge Inception Voltage
- THD: Total Harmonic Distortion
- VFT: Very Fast Transient
- VSC: Voltage Source Converters

List of figures

List of tables

INTRODUCTION

The number of electronic converters in the power system is already considerable, but expectations are that this number will increase dramatically with the gradual implementation of the smart grid paradigm. Applications of electronic converters include, e.g., motor drives, reversible generator drives, wind turbine/grid interfaces, HVDC links based on Voltage Source Converters (VSCs). It is interesting to observe that the voltage level of these equipments ranges from 400 V to hundreds of kV. In other words, converters are spreading at all voltage levels and interact with all types of equipment: motors, generators, cables, transformers and inductors.

Since the very essence of converter technology consists in turning on/off semiconductor switches, converters are known to cause voltage surges with steep fronts. This surges travel on cables or overhead lines and are often reflected at some point of the network due to impedance mismatches (e.g., at a cable/induction motor interface), giving rise locally to overvoltages. Furthermore, high slew rates cause uneven turn voltage distribution in inductive components and thereby expose the insulation of power apparatus to electric fields which can be considerable higher than those at power frequency. Phenomena that are typically associated with these overvoltages are partial discharges, heating and possibly space charge accumulation in the dielectric. All of them contribute to insulation system degradation.

The main scope of this document is a) to review the definitions for fast repetitive transients, b) discuss the root causes of degradation and their influence on electrical insulation endurance and, c) providing a review of relevant test methods for determination of the endurance of materials and apparatus under repetitive transients.

The approach will be based on both insulation materials and apparatus types to be exposed like, e.g., rotating machines, transformers and cables. Measurement techniques, like partial discharges or space charges under transients, will not be covered.

DEFINITIONS

An overview of different types of transient voltages is given in IEC 60071 *Insulation co-ordination* standard [1], including switching, lightning and very fast transients (VFT), each of those described by a number of parameters. The endurance of solids under transients will be dependent on the different parameters and in the following an overview of the standardized definitions of the parameters is provided.

The most obvious parameters to describe a pulse are magnitude, pulse shape and repetition rate. Regarding shape and magnitude, IEC 60060 [2] defines some standard quantities to be used for testing purposes: pulse magnitude, rise time t_r (also called t_1) and half value time t_{50} (also called t_2), see Figure 1. Typical rise time values are [3]:

1) t_r = 20-5000 μs for switching events
2) t_r = 0.1 – 20 μs for lightning
3) t_r = 3-100 ns very fast transients.

These phenomena can be sporadic, as e.g. lightning and switching events or repetitive, as VFTs generated by power converters. In particular, VFTs occur in case of power converters (having 2, 3, etc… levels) working with either MOSFET or IGBT as switching devices. In both cases, rise times are in the range of typically 20 to 200 ns [4].

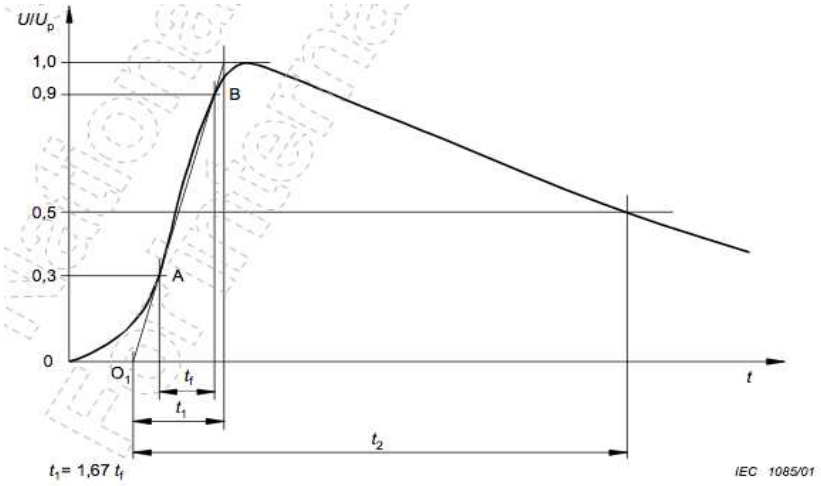

Figure 1.**IEC 60060 Standard pulse shape [1]**

With respect to the transients described in IEC 60071, VFTs created by power converters at motor/generator terminals usually have a waveform which cannot be described by the simple shape in Fig 1. Bearing in mind reflection phenomena associated with impedance mismatch and resonances, IEC 60034-18-41 and IEC 60034-18-42, [5][5][6] provide a more specific description of these events through the standard waveform reported in Figure 2. The parameters describing this standard pulse shape are:

- U_p= peak voltage: maximum impulse voltage value reached during a unipolar impulse (for bipolar impulse, it is half the peak to peak voltage).
- U_b= voltage overshoot: magnitude of the peak voltage in excess of the steady state impulse voltage.
- U_a= steady state impulse voltage magnitude: final magnitude of the voltage impulse.

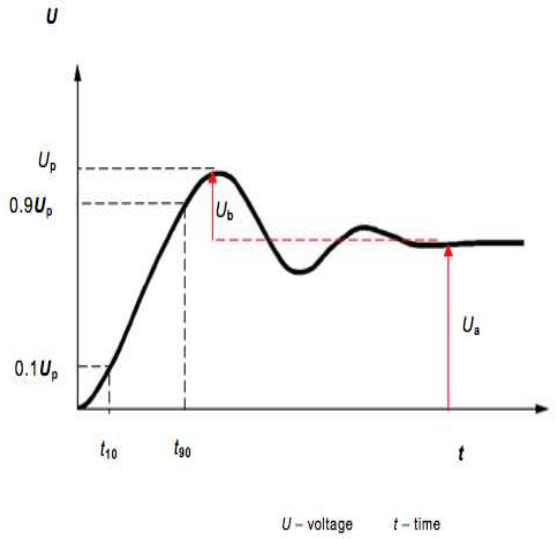

Figure 2.**Definition of front of voltage pulse from voltage converters [5]**

From Figure 2, it can be seen that the rise time is defined as 10-90 % for this type of pulses. For rotating machines, typical values are reported in Table 1. The specific values will depend on the insulation type (hence on voltage level and, therefore, on switch type). For random-wound (low voltage) coils, typical values for rise time are t_r=50 ns– 200 μs, impulse repetition rate f_{rep}=100 Hz–20 kHz, and impulse durationt_d=10 μs-1ms [5].

Form-wound (mostly medium voltage) coils, are generally subjected to voltage waveforms with longer rise times and lower repetition frequencies, due to the larger voltage levels which limit switch turn on/off capability.

Table 1. Common ranges of characteristics of the terminal voltages of converter fed machines [7]

Characteristics	Range of values
Peak/peak impulse voltage	0.5 to >5 kV
Peak/peak voltage	1.0 to >10 kV
Impulse rise time	0.1 – 10 μs
Impulse voltage repetition rate	100 – 20 000 Hz
Impulse duration	10 – 10 000 μs
Shape	Rectangular
Polarity	Unipolar or bipolar
Fundamental frequency	5 – 1000 Hz
Mean time between impulses	≥ 0.6 μs

For transformers, little information is available on the type of voltage impulses. One of the most severe applications will be the high or medium voltage interface between the grid and wind farms realized through two-level inverters. Bearing this in mind, an estimate could come from the data sheets of commercially available medium voltage IGBTs. Data sheet show that units having a collector-emittar voltage, V_{CE}, up to 4 kV, collector current, I_C, up to 1.5 kA have rise and fall times of >0.5 μs, an operating frequency in the range of 1-3 kHz. For higher voltages, no explicit information could be found.

It is important to notice that converter operation is characterized by the carrier and modulating (or fundamental) frequency. The number of surges per second (hence, the stress on the component connected to the inverter) will be equal to the carrier frequency (see Figure 3). The modulating frequency will affect the possibility that space charge is injected at electrode boundaries: lower modulating frequencies will favour space charge formation [7].

It is also important to observe that different voltage waveforms will be applied to different parts of the insulation system which can be ideally split into 1) phase/phase, 2) phase/ground, 3) turn/turn insulation system. A typical waveform of phase/phase voltage produced by a 3-level converter is shown in Figure 4. Figure 5 shows the corresponding line-to-ground voltage highlighting the so-called jump voltage, i.e., "*change in voltage at the terminals of the machine occurring at the start of each impulse when fed from a converter*" [5]. Figure 6 shows a schematic representation for phase/phase, phase/ground and turn/turn voltages. The voltage stressing the turn insulation will be a fraction, α, of the jump voltage.This fraction will depend on winding design and will become larger as the rise times get shorter as explained in the next Section.

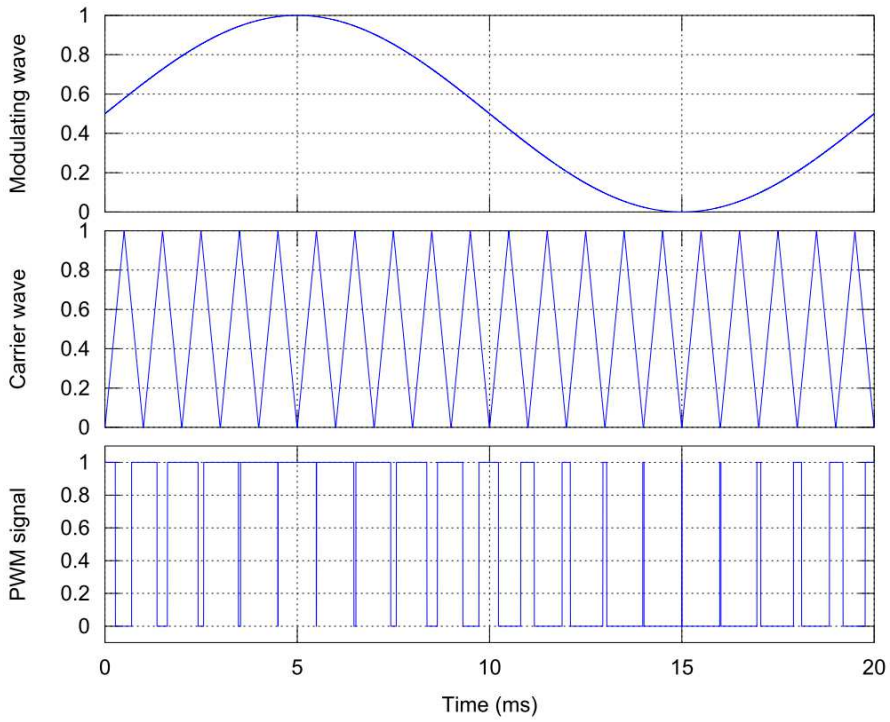

Figure 3.**Example of modulating (top) and carrier (middle) waves, PWM signal (bottom)**

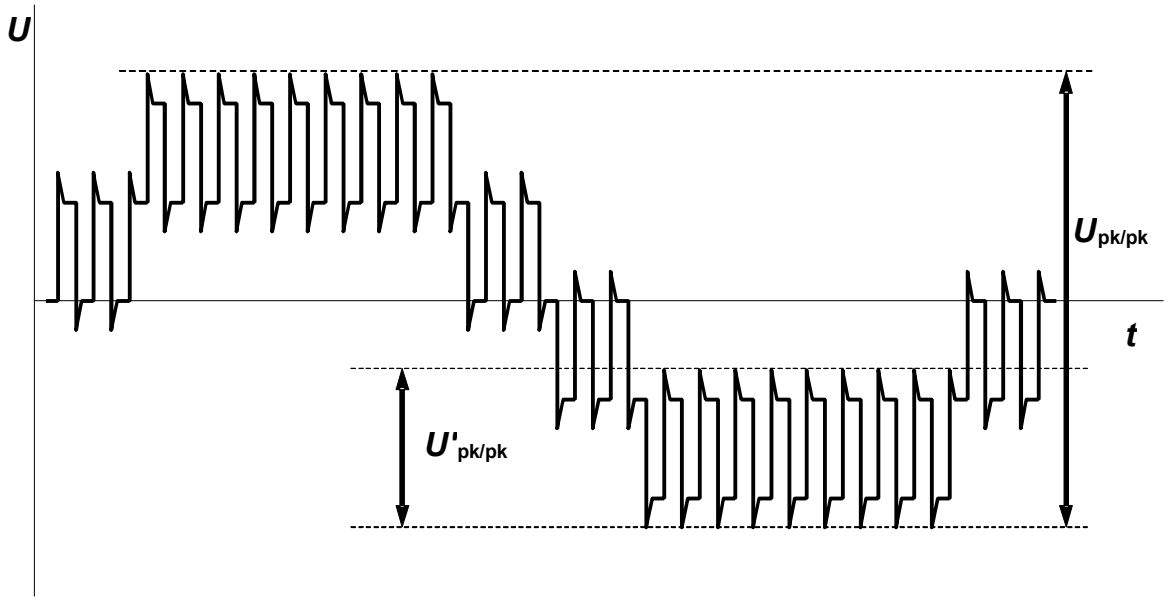

Figure 4.**Phase/phase voltage at the terminals of a machine fed by a 3-level converter [5]**

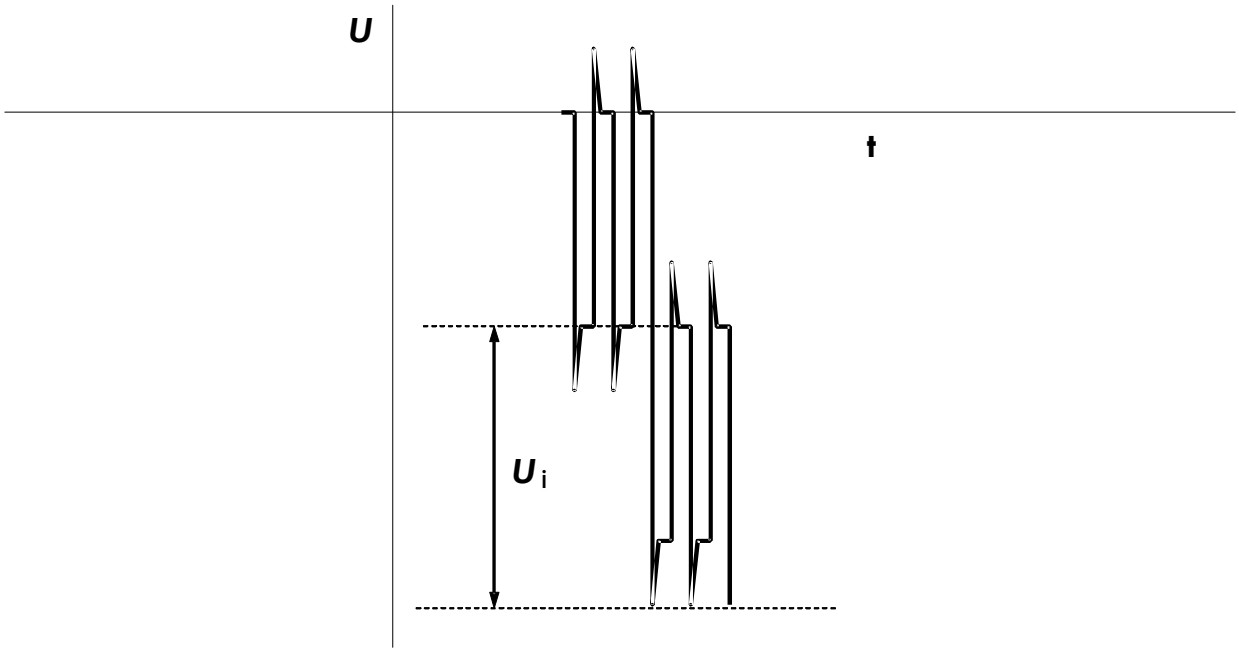

Figure 5.**The jump voltage (Uj) at the machine terminals associated with a 3-level converter drive [5]**

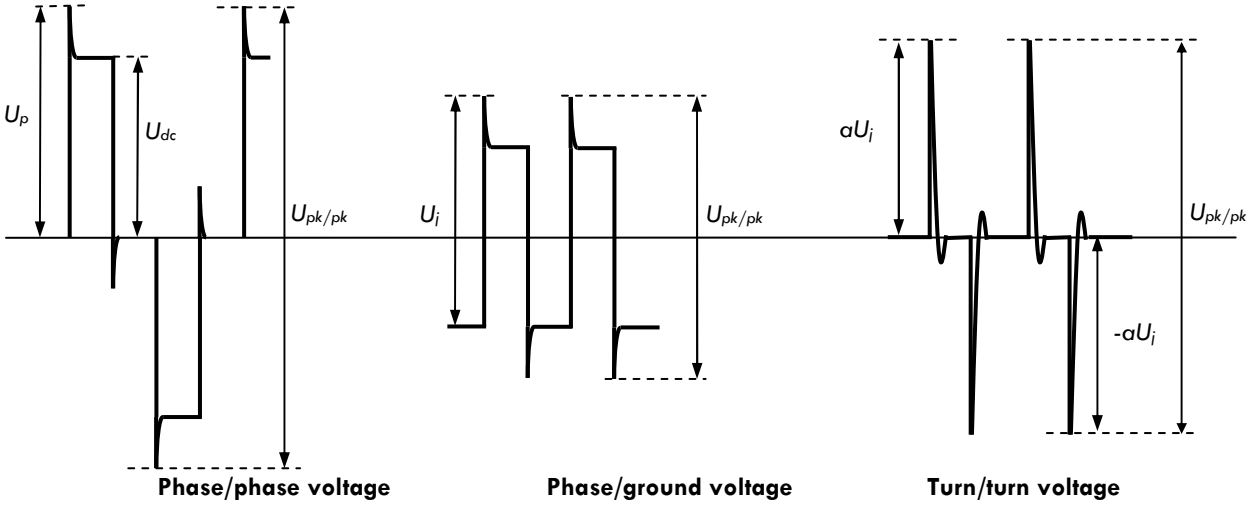

Figure 6.**Comparison of phase/phase, phase/ground, and turn/turn voltages for a 2-level converter. [5]**

STRESS ENHANCEMENT PHENOMENA

Electrical stress

When dealing with electrical stress, two phenomena must be accounted for when a converter supplies an EUT: the reflections occurring at the EUT terminals and the fact that the electric field distribution can considerably depart from that at 50/60 Hz AC. Both phenomena are particuarly important for inductive devices as rotating machines, inductors and transformers [8]- [13].

Reflections

Reflection phenomena take place whenever a surge travelling on a transmission line reaches a point where the characteristic impedance of the system changes abruptly. This is typically the case of inverter surge travelling on a cable and reaching an inductive winding. The cable characteristic impedance is in the range of a few tens of Ohms, whereas that of the machine is generally hundreds of Ohms, as depicted in Figure 7. As a result, the reflection coefficient

$$\Gamma = \frac{Z_{0,winding} - Z_{0,cable}}{Z_{0,winding} + Z_{0,cable}} \approx 1 \quad (1)$$

is often close to unity, and the peak voltage of the surge is doubled at the winding termination. As the inverter can be regarded as a short circuit, the surge traveling back to the inverter is reflected again towards the winding with a negative Γ coefficient:

$$\Gamma = \frac{Z_{0,inverter} - Z_{0,cable}}{Z_{0,inverter} + Z_{0,cable}} \approx \frac{-Z_{0,cable}}{Z_{0,cable}} = -1 \quad (2)$$

re-establishing the voltage to that of the DC bus voltage. The exact magnitude of the overvoltage will depend on the surge rise time, cable length and propagation speed (160-180 m/μs). An approximate solution is reported in Figure 8, [14]. Note that, if the switch closes and opens in a very short time, the surge arrives at the inverter when the switch is again an open circuit and is thus reflected towards the winding with Γ=1. Under this peculiar condition, the total overvoltage can reach about three times the DC bus voltage.

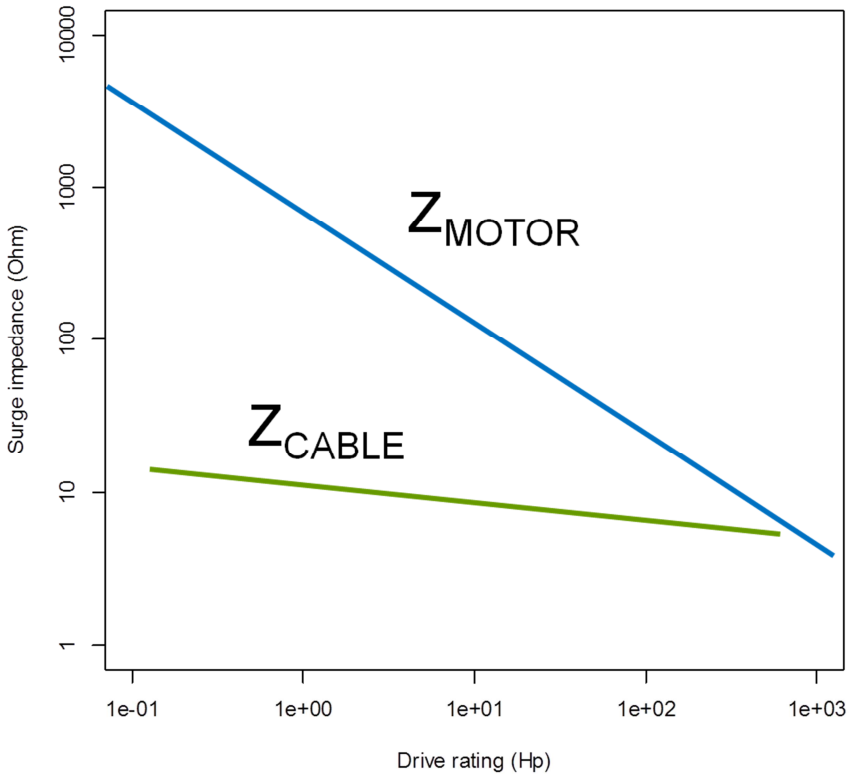

Figure 7. **Qualitative relationship between surge impedance for cables and motors as a function of motor ratings in hp**

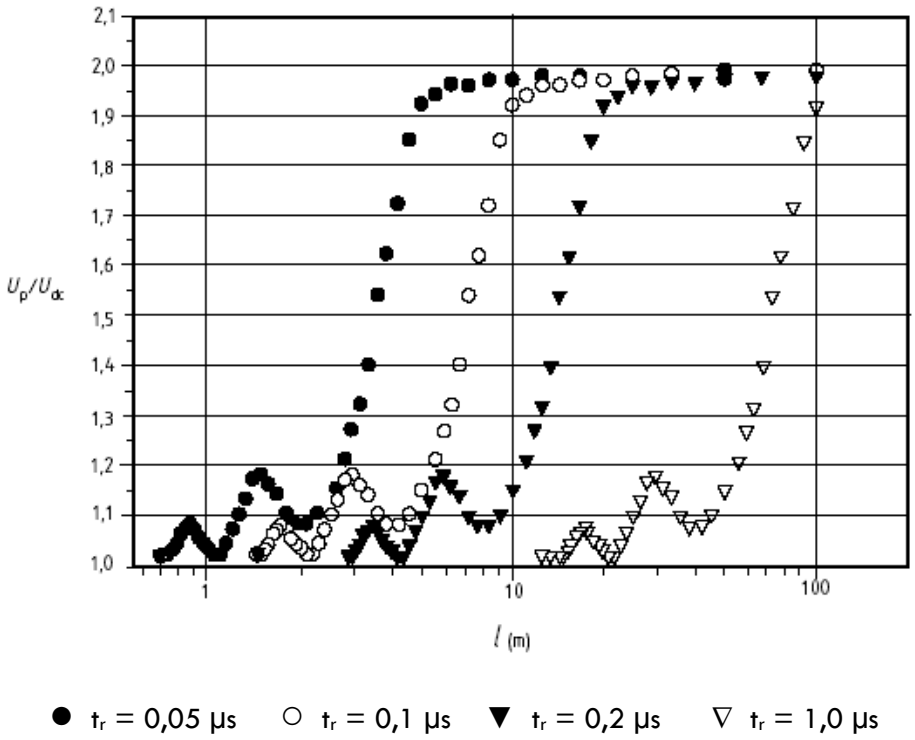

Figure 8.**The jump voltage (Uj) at the machine terminals associated with a converter drive**

Uneven distribution of turn voltages

A closer look at the voltages in an inverter fed machine with ungrounded star center is provided by Figure 9 and Figure 10. Figure 9a shows the line-to-line voltage. The surges have comparable magnitudes, except for the slight modulation of the bus voltage. Figure 9b shows that, on the contrary, the line-to-ground voltage (where ground reference is taken on the stator frame), shows a larger variability associated with the floating potential of the star center.

Observing with a shorter time scale, the electric signals of Figure 9 highlight pulses having different shapes due to the aforementioned modulation of the star center, and interferences from commutations in other phases (Figure 10a). A further zoom highlights ringings at a frequency of about 2MHz (Figure 10b).

If the turn voltage distribution has to be investigated, it is important to observe that the equivalent circuit of the winding is very complex and random in nature [15]-[19] A simplified representation is reported in Figure 11, where the winding is modelled as a cascade of cells consisting of:

- The series and mutual inductance of each turn in a coil.
- The series resistance of each turn.
- The turn/turn capacitance of each turn with respect to adjacent turns
- The turn/ground capacitance of each turn

Similarly to what happens in transformers subjected to lightning impulses, the turn voltage distribution is not expected to be even during the transients induced by the impinging voltage sources. On the contrary, most of the line voltage will be applied to the first few turns, thus raising the electrical stress of the turn insulation.

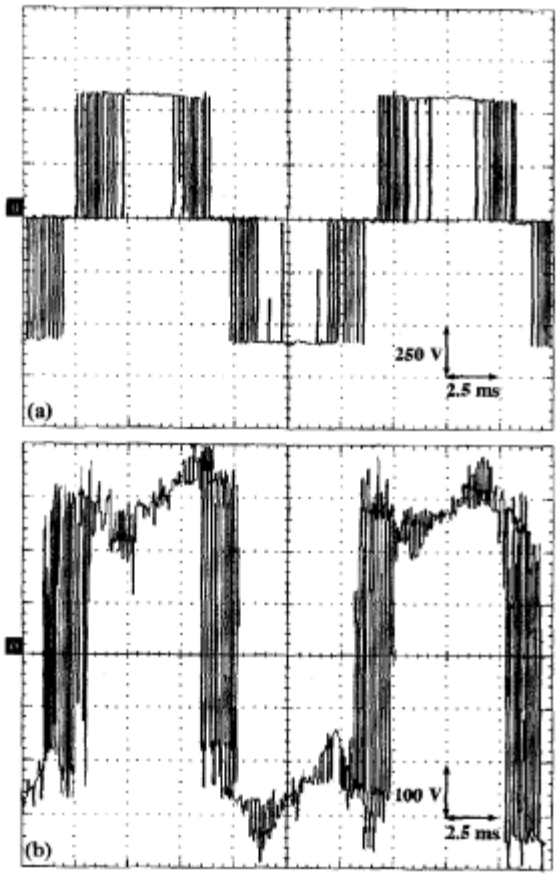

Figure 9. Voltages at motor terminals, after [10]: a) line-to-line and b) line-to-ground voltages

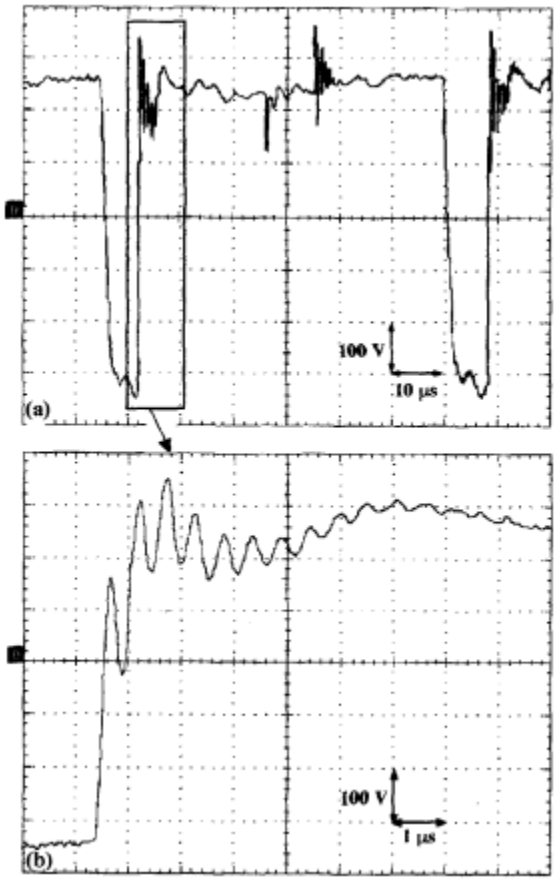

Figure 10. Voltages at motor terminals, after [10]: details of line-to-ground voltage.

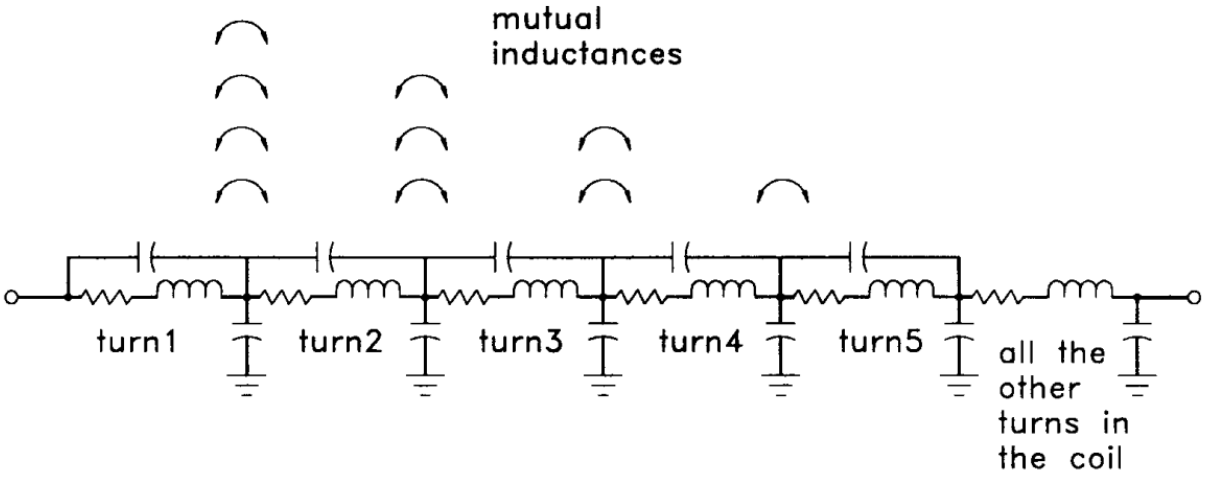

Figure 11. Equivalent circuit for an inductive EUT

Lebey et alii measured the turn voltages and the potential difference between (electrically) adjacent turns using a motor with accessible turns, see Figure 12. They confirmed that the voltage distribution between turns is not linear, being the first couple of turns the one that must whitstand most of the voltage. In addition, ringings were observed only in the first turn. For random wound motors, models to predict the actual turn voltage distribution are hard to derive and inherently probabilistic. In the absence of specific knowledge, the maximum value of the interturn voltage can be estimated through the worst case curve provided in Figure 13 and reported in [5]. For transformers and medium voltage machines (form wound coils), FEM software can be used to derive the exact turn voltage distribution.

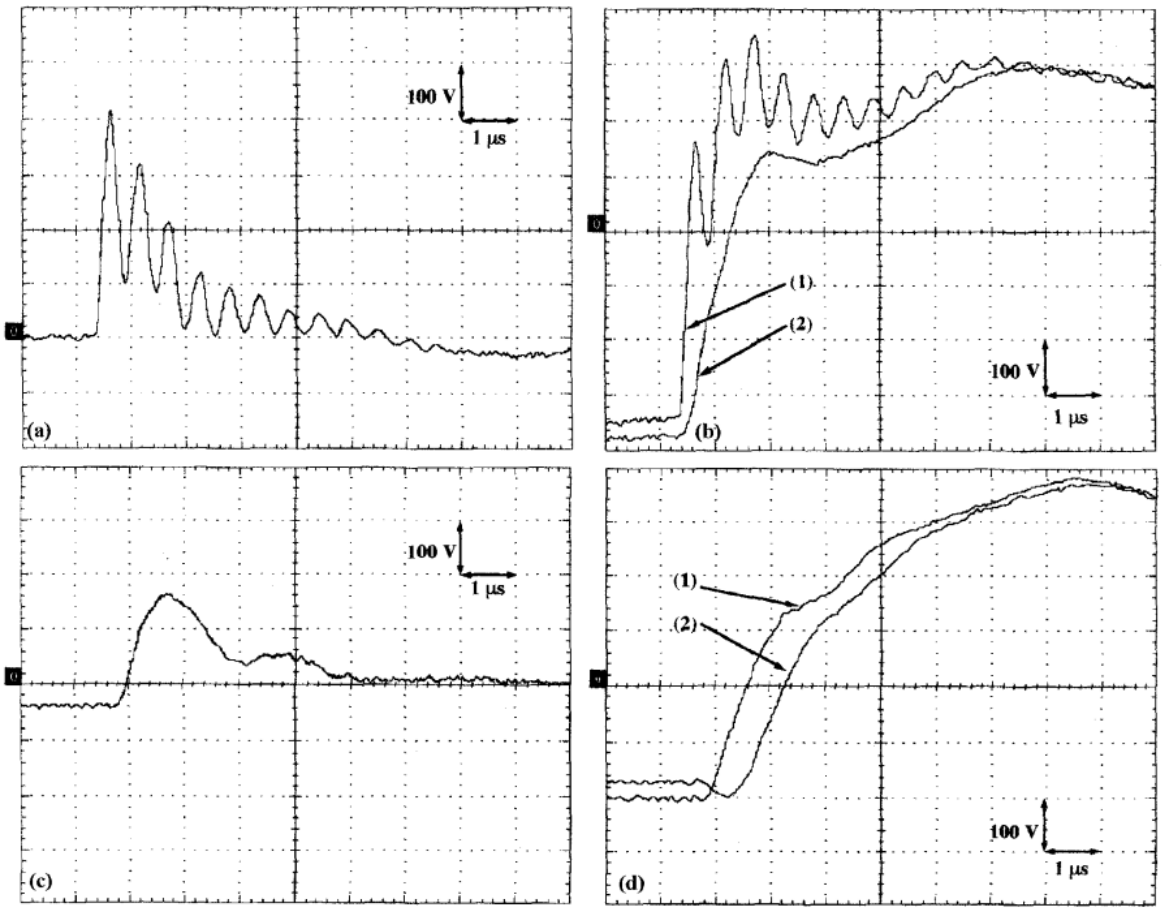

Figure 12. **Turn voltages , (a) Potential difference between first couple of turns, (b) Turn voltages in the first two turns, (c) Potential difference between a subsequent couple of turns, (d) Turn voltages in subsequent turns. (after [10]).**

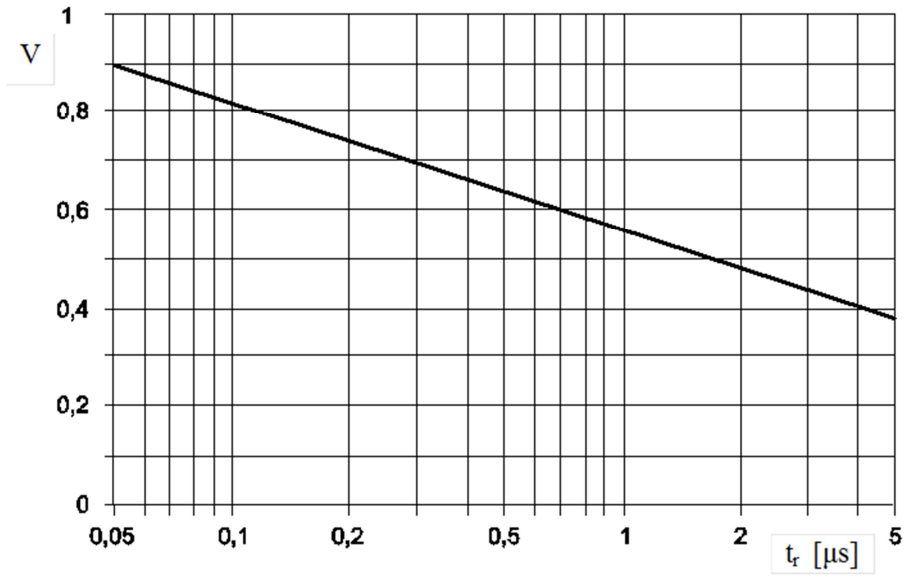

Figure 13. **Fraction of the jump voltage that, in the worst case, is actually applied at the turn insulation [5]**

Thermal stress

Dielectric heating

Dielectric heating is enhanced by converter square voltage waveforms since their frequency content largely exceeds that of 50/60Hz AC waveforms. Dielectric losses for a pure sinusoidal waveform are given by:

$$P_D = \omega_1 C V^2 \tan\delta \tag{3}$$

where V and ω_1 are the magnitude and the angular frequency of the applied voltage, C is the capacitance of the insulation system, tanδ is the loss angle of the insulation.

When multiple harmonics are considered, the total losses will be given by the sum of the losses at each harmonic frequency:

$$P_D = \sum_{h=1}^{n} P_h = \sum_{h=1}^{n} h\omega_1 C_h V_h^2 \tan\delta_h \tag{4}$$

where h is the harmonic order, the other quantities are as in the previous equation, but evaluated at each harmonic order.

Eventually, it is possible to evaluate the increment in power losses with respect to the fundamental component (DP) as:

$$DP = \sum_{h=1}^{n} P_h P_1 \tag{5}$$

Assuming that C_h and $\tan\delta_h$ are independent of frequency, then [20]:

$$DP = \sum_{i=1}^{n} h(V_h/V_1)^2 \tag{6}$$

For a modulating frequency of 50 Hz, and a variable carrier frequency up to 10 kHz, the DP values are those reported in Figure 14, which shows that dielectric losses can dramatically increase as a function of carrier frequency.

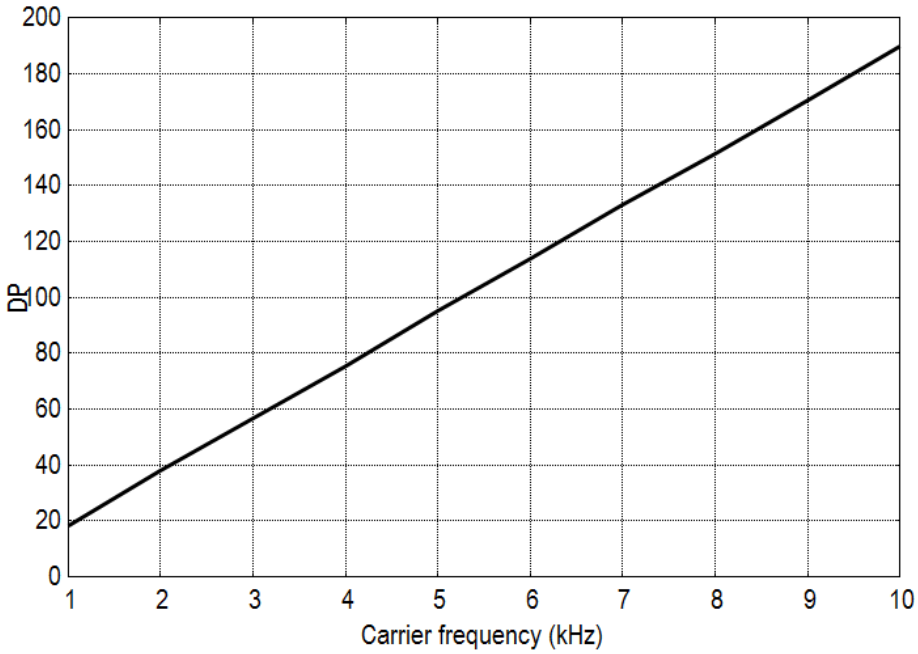

Figure 14. **Increase of dielectric losses as a function of the carrier frequency for a 50 Hz modulating waveform.**

For paper/oil insulation systems, dielectric heating could explain why these systems tend to exhibit lower PDIV values. In fact, as higher temperatures can give rise to higher gassing rates of the oil trapped in the paper pores.

Magnetic core losses

Due to the large frequency content, PWM waveforms also rise losses in the magnetic core. In fact, hysteresis and eddy current losses increase with the frequency, f, of the voltage waveform:

$$W_{hystesresis} = K_h \cdot f^{1-1.5} \cdot B_m^{1.6} \tag{7}$$

$$W_{eddy\_current} = f^{1.5-2} \cdot K_f^2 \cdot B_m^2 \tag{8}$$

where the actual exponent of the frequency will depend on the thickness of the laminations, through the skin losses.

As an analytical treatment is quite difficult, to quantify the increase in iron losses Boglietti et alii [21][22] measured the iron losses directly and compared those obtained under sinusoidal, (six-step) square waves and PWM waveforms. The results are reported in Figure 15, which show that iron losses can increase by a factor of

approximately 2 using PWM converters. It is important to observe that these measurements were carried out during the 90s of the last century, using square waves of relatively low frequency (1070 Hz) compared to those used to date (from 10 to 20 kHz). Thus, one should expect even larger iron losses in present day drives.

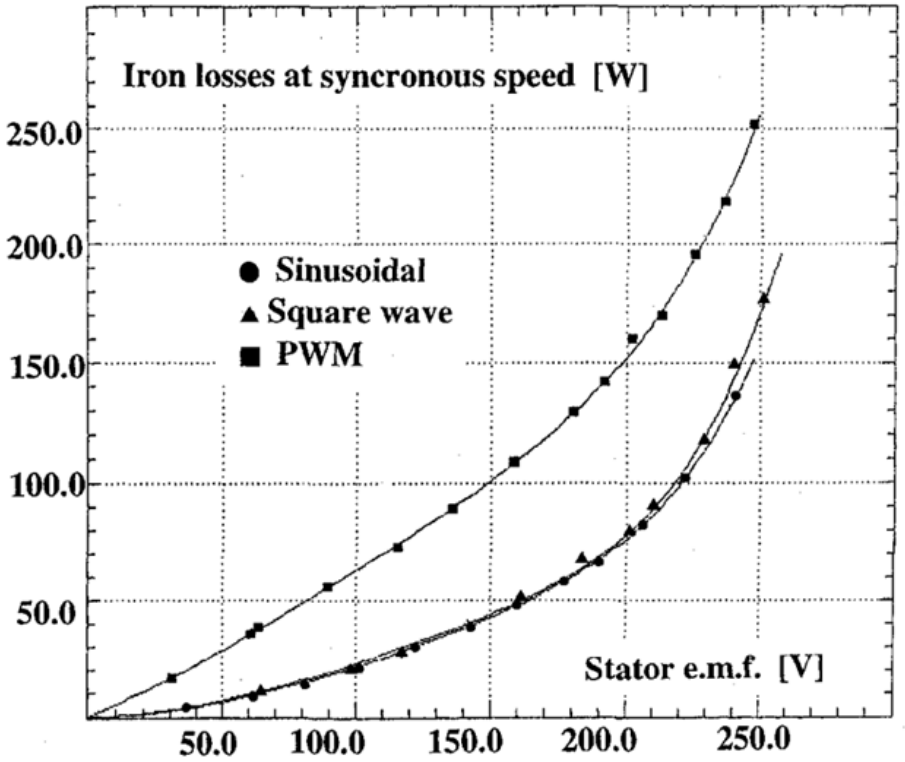

Figure 15. **Iron losses versus fundamental supply voltage at synchronous speed with sinusoidal, six-step, and PWM inverter sources (Material: Si-Fe, fundamental frequency of 50 Hz, switching frequency of 1070 Hz) [21]**

Stress grading losses

The large capacitive currents associated with the application of repetitive voltage surges to insulation systems, might induce hot spots in the partially conductive coatings used to grade the electrical stress at the end-windings of rotating machines or cable terminations. If these systems are designed bearing in mind that the equipment has to work in a power electronic drives, the hot spot temperatures are generally acceptable. However, if the grading system has been designed to operate under 50/60 hz sinusoidal voltages, the hot spot temperature can become significant, and trigger thermal ageing of the grading itself. This will be discussed in more detail further on.

AGING AND BREAKDOWN

General overview

The detrimental effects of repetitive surges on a number of insulation systems have been reported in several references (see e.g. [23]-[36]). A clear picture of the relation between pulse parameters and breakdown can be derived synthetizing some results from [23] which deal with the insulation system typically used for standard low voltage motors. Figure 16 shows the number of impulses to breakdown measured as a function of impulse amplitude and polarity for a motorette (i.e., an insulation model). The motorette was made a dip-impregnated coil, 2 cm in diameter, consisting of two polymide enamel-insulated, parallel-wound wires of 2 m in length. These coils were used with open ends; thus, the insulation was evenly stressed with the terminal voltage. A photomultiplier tube was used to detect the presence of partial discarges (PD), and PD inception probability

was calculated as the ratio of the measured voltage pulse number with PDs and the number of applied voltage pulses.

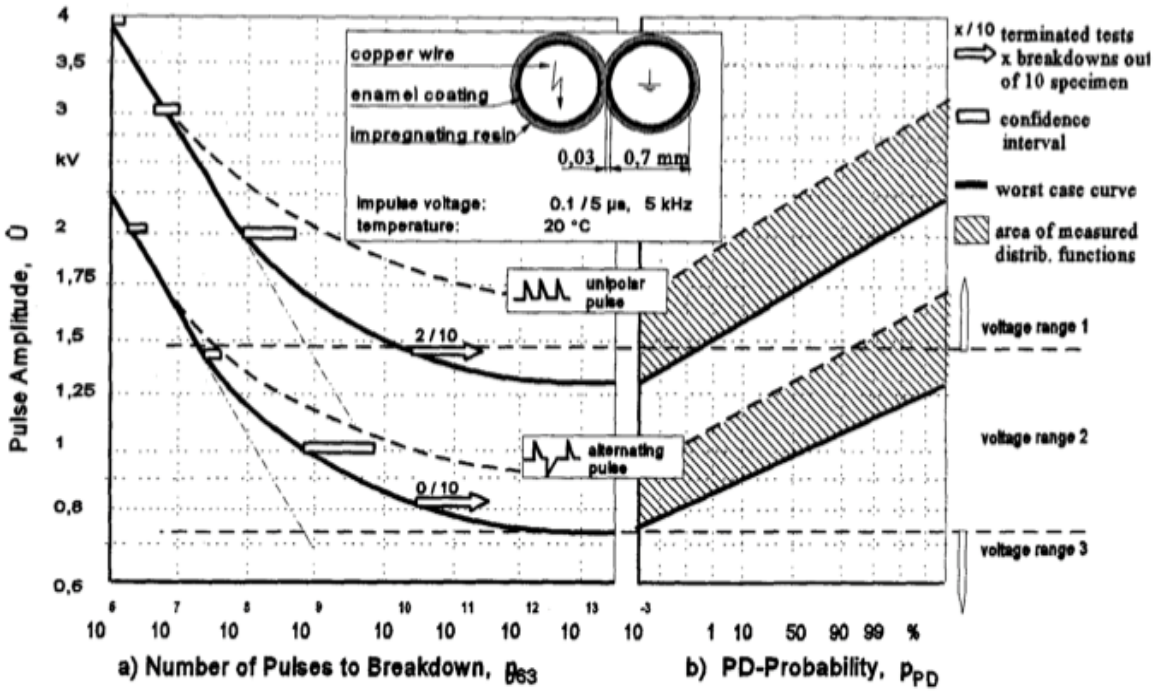

Figure 16. **Endurance tests of model coils: a) number of pulses to breakdown and, b) PD inception probability as a function of applied voltage. [23]**

It was found that the number of impulses to breakdown strongly decreases with increasing voltage impulse amplitude. This dependence was readily explained observing the PD inception probability plots on the right. The conclusion was that, above 700 V, PD activity incepted in the insulation was the main cause of accelerated degradation.

These results were in line with theoretical considerations based on the comparison of the electric field at the conductor boundaries and the breakdown field E_{BD} of a gap having length d. The breakdown field was evaluated through the Paschen law as:

$$E_{BD} = \frac{a \cdot p}{\ln(p \cdot d) + b} \tag{9}$$

where $a=4.36 \cdot 10^7$ V/(atm·m), b=12.8 (assuming the field constant over the field lines). Figure 17 shows that, for the specific case dealt with, the minimum inception voltage should be around 700 V (i.e., the PD inception limit as observed experimentally): at this voltage level, the air gap will break down along field lines having a length of 20 µm. At higher voltages, longer field lines can break down and, therefore, the area of enamel fulfilling the discharge criterion increases, thus PD probability becomes larger.

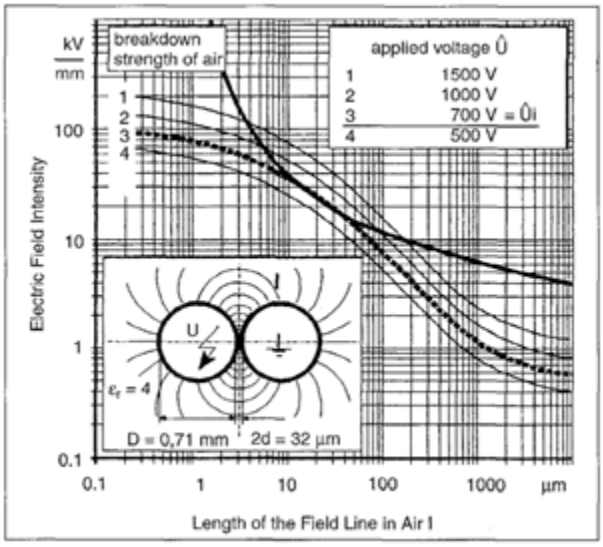

Figure 17. **Comparison of field lines in the air gap with the Paschen law (thicker line) [23]**

This result was used to explain how geometry and material properties could help to explain the different endurance of systems having different characteristics (Figure 18 and Figure 19). By comparisng the lifetime of four different interturn insulations it comes out that the thicker the insulation layer and the better the impregnation, the longer the lifetime and the higher threshold voltage of the ageing (i.e., the higher the voltage required to incept PD).

In addition, Figure 20 shows the influence of temperatures on PDIV. Compared with room temperature, the PD inception voltage decreases by 15% by increasing the temperature. This is due to the higher permittivity of the polyimide at higher temperatures, which can be confirmed indirectly by the increased specimen capacitance, which eventually leads to higher electric field intensities in the air gaps. Also, the breakdown strength of air decreases at higher temperatures because of its lower density. Therefore, besides the thermal ageing, higher temperatures lead to a thermally accelerated electrical ageing of the interturn insulation.

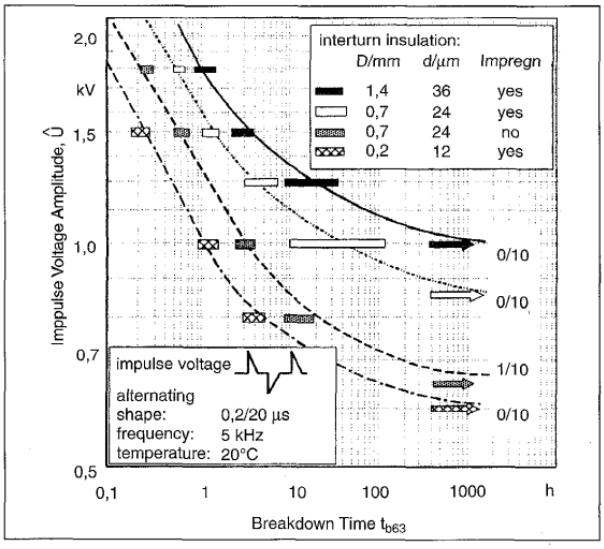

Figure 18. **Endurance of wire wound coils with different wire geometries [23]**

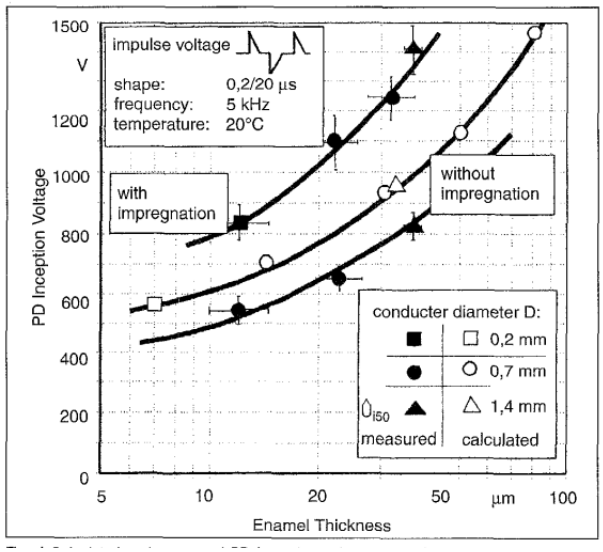

Figure 19. **Endurance of wire-wound coils as a function of enamel thickness.**

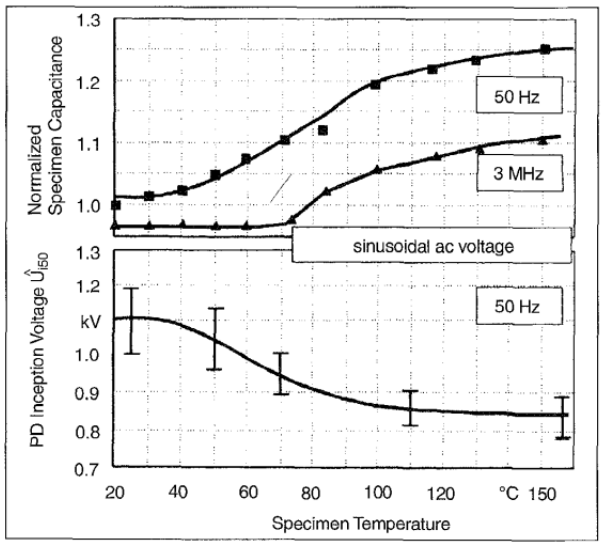

Figure 20. **Wire-wound coil capacitance as a function of frequency and at different frequencies (above), PDIV as a function of temperature (below)**

Intrinsic aging

As noted above, partial discharges are generally the most harmful degradation process. However, even in the absence of PD, intrinsic aging takes also place, and its effects are more marked when high frequency voltage waveforms are employed.

As an example, Figure 21 shows lifetimes of twisted pairs obtained at different frequencies and different voltages [14]. The twisted pairs were immersed in silicone oil to prevent PD inception. It can be appreciated that lifetimes are much shorter when using high frequency sinusoidal waveforms.

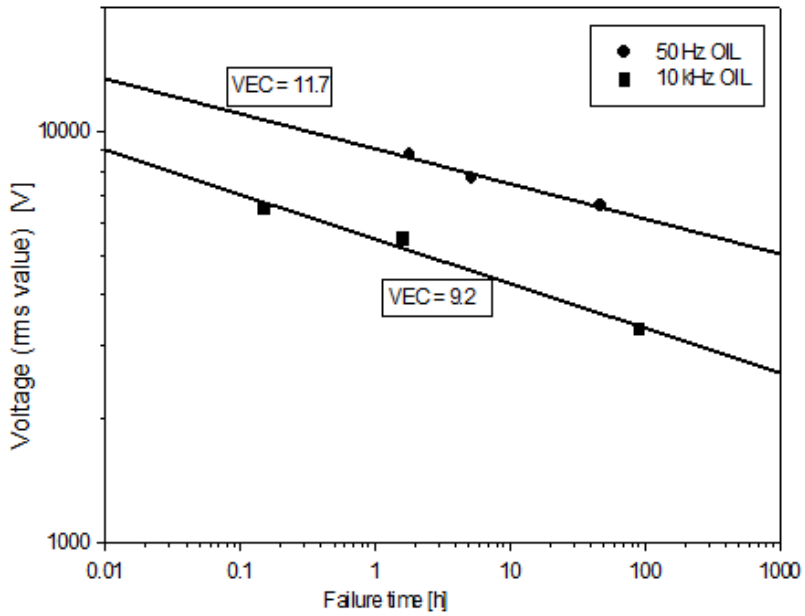

Figure 21. **Lifetime of twisted pair at different frequencies and voltages. Twisted pair were immersed in oil to prevent PD inception.**

These results, together with others from literature, suggest that, similarly to mechanical fatigue, the average number of cycles to breakdown, N_{cycles}, is independent of frequency. Thus, a frequency-scaling rule can be used to extrapolate breakdown times at different frequencies:

$$N_{cycles} = f_1 \cdot t_1 = f_2 \cdot t_2 \tag{10}$$

where N_{cycles} is the number of cycles to breakdown, f_1 and t_1, f_2 and t_2 are two different surge frequencies and the corresponding breakdown times. Indeed, it has been observed that intrinsic aging is a minor effect if compared with PD activity.

Partial discharges

For solid insulation systems, the root cause for breakdown is often the inception of partial discharges (PD). Under repetitive surges, above the PD inception voltage (PDIV) PD activity is almost continuous, with generally a PD event on each rising flank and one on each falling flank of the voltage waveform [23]. As an example, for a converter operating with a carrier frequency of 10 kHz, it is quite likely to have roughly 20000 PD events per second. If compared with 50 Hz supplies, where the number of PD is a few hundred per second when much, the degradation under PWM waveforms can be extremely severe. Furthermore, PD magnitudes are larger when using square waves with short rise times if compared with those obtained using 50 Hz AC waveforms [**14**]. Thus, the degradation effect can be remarkably fast. In the following, we shall discuss in more detail the dependence of PD on impulse voltage parameters.

Effect of surge polarity

During a PD event, charges (mostly electrons and positive ions) are left at the gas/dielectric interface. When, due to these charges, the local field drops to the so-called residual field, E_{res}, the discharge extinguishes spontaneously. These charges prevents the immediate reignition of another PD. However, as time elapses, they migrate on the surface and in the insulation body. Consequently, the electric field starts to increase again so that new PD events can take place. If new PD do not occur, after a sufficiently long time the local field matches again the external field. Therefore, this charge does constitute the memory of the system and has a deep influence on the development of PD, particularly under converter waveforms, where the time between turning on and off of the applied voltage are so short that memory can be assumed as infinite (i.e., on practical grounds, the charges can be considered as permanent).

Let us consider what happens in a system subjected to unipolar square waves when the peak local field slightly exceeds the inception field, E_{inc} (see Figure 22a). As soon as a starting electron becomes available, a PD is incepted. Consequently, the field drops to E_{res} or, in other words, the space charge due to PD creates a charge field (with sign opposite to the background field) equal to E_{inc}-E_{res}. After the PD event, as long as the external voltage has the same value, the local field will be equal to E_{res} (hypothesis of infinite memory). When the voltage drops to zero, the field will drop to E_{res}-E_{inc}, i.e., still below the inception field in absolute terms. Due to recombination phenomena, after a sufficient long time, the charge left by the PD event will recombine, and condition for ignition will be met again. This process, however, could take several milliseconds.

For bipolar waves, after the PD occurrence, as soon as the voltage reverses, the conditions for a new PD event are met since the local field may exceed largely the inception field (see Figure 22b).

Unipolar and bipolar waves will have the same effect (in terms of number of discharges per period and discharge magnitude) if the unipolar and bipolar waves are comparable in terms of peak-to-peak voltage (see Figure 23).

These speculations are supported by accelerated life tests performed on twisted pairs [**14**][24][25][26] and highlight that peak-to-peak voltages should be considered. In particular, Figure 24 shows how the lifetimes of

twisted pairs can be predicted by the same model if the applied voltage is reported in terms of peak-to-peak voltage.

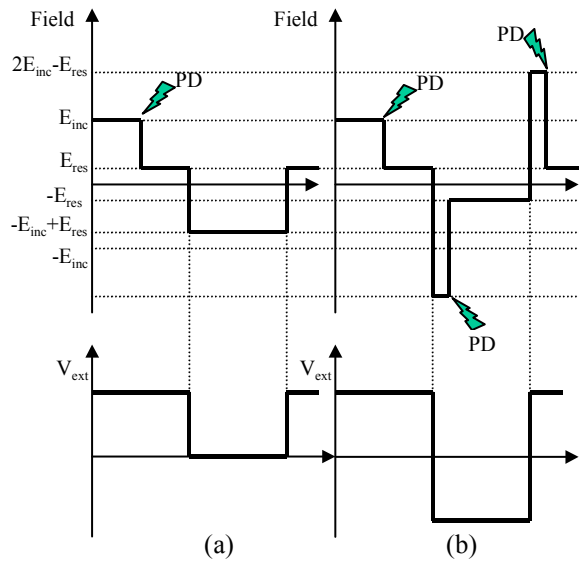

Figure 22. **Evolution of the local field after a PD and close to the inception voltage for a long-memory system subjected to a unipolar square wave (a) and for a long-memory system subjected to a bipolar square wave (b).**

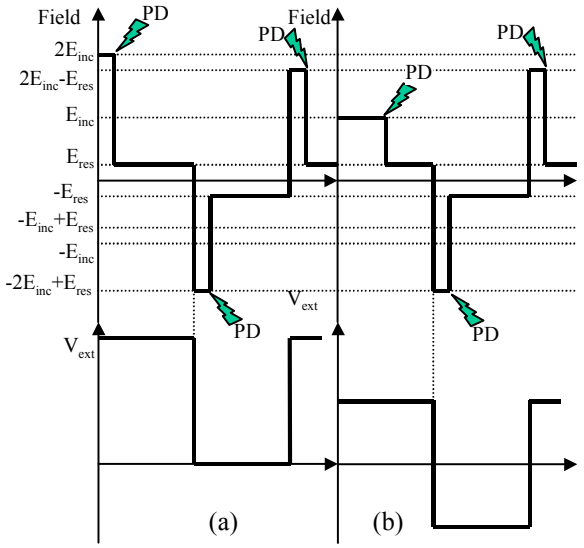

Figure 23. **Evolution of the local field in two systems, one (a) subjected to a unipolar square wave having amplitude equal to two times the inception field, the other one (b) subjected to a bipolar square wave having amplitude equal to the inception field. System with infinite memory.**

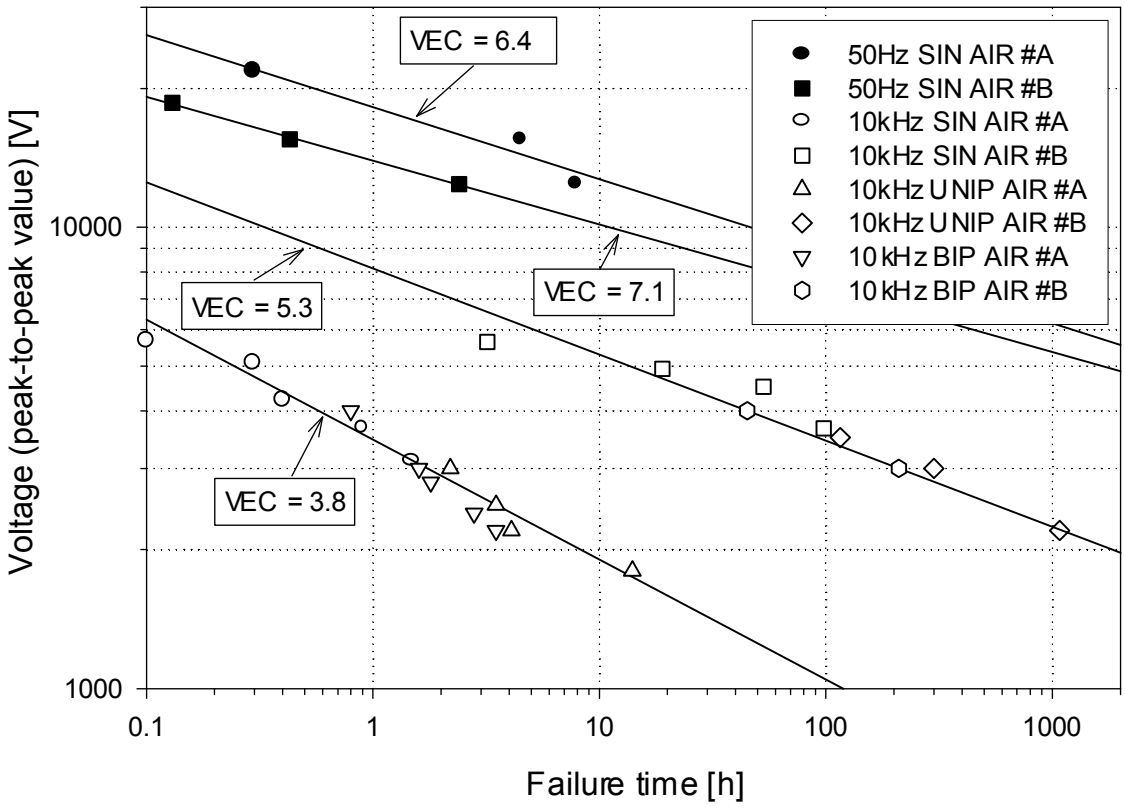

Figure 24. **Lifetime of crossed enameled wires as a function of peak-peak voltage [14].**

Repetitive Partial Discharge Inception Voltage (RPDIV)

The above discussion suggests that there exists a difference between the voltage at which a PD becomes possible (Partial Discharge Inception Voltage) and the voltage at which PD can be observed almost continuously in the EUT. The difference depends on voltage waveforms, the dependence being particularly striking when unipolar or bipolar voltage waveforms are considered.

In practice, the estimate of the true PDIV for unipolar square waves could be affected by large errors, since a single isolated PD event could be easily misinterpreted as noise or going unnoticed.

In order to solve these practical problems, reference should be made instead to a new quantity known as Repetitive Partial Discharge Inception Voltage (RPDIV), defined as *the minimum peak-to-peak voltage at which PD occur with a mean repetition rate of 1 or more PD pulses for every 2 voltage impulses averaged over the specified test time. The voltage applied to the test object is gradually increased from a value at which no PD can be detected* [5].

It is worth noting that RPDIV for unipolar and bipolar waves is almost the same, in terms of peak-to-peak voltage.

Effect of rise time

When the voltage is turned on, it takes a finite time (as a first approximation, the dc bus voltage divided by the switch slew rate) to reach its maximum. During this time it is possible to assume that the voltage increases linearly until the field is large enough for PD inception. However, the PD is incepted only when a starting electron becomes available. Therefore, there is a statistical delay between the moment the voltage is sufficient for PD inception and the moment the PD is incepted. Hence, the PD is generally incepted at a higher voltage that the PDIV (see Figure 25). Consequently, depending on the slew rate of the device, the overvoltage can become important, and the PD magnitude could increase in an appreciable way.

These speculations were corroborated by (a) PD magnitude measurements, (b) accelerated life tests. As an example, Figure 26 (from reference [**37**]) shows that, the shorter the rise time, the larger the PD magnitudes. The dependence on rise time is remarkable. This has an obvious effect on insulation lifetime that generally decreases with voltage impulse rise time, as shown in Figure 27, [**37**]. Indeed, given the difference in PD magnitudes between sinusoidal and square waves (particularly those with rise time $\leq$1 μs), one would expect a much longer lifetime under sinusoidal voltages. To explain this one should consider that:

1) Besides PD bombardment, chemical attack (ozone and weak acid are created by the interaction of PDs with air and the polymer) is also an important degradation factor. Chemical attack might be less tied to PD magnitudes.
2) Under longer rise times or sinusoidal voltages more PD events can take place (see Figure 28).
3) Intrinsic ageing is also active.

These considerations, together with those presented earlier concerning uneven turn voltage distribution and voltage reflections under steep-fronted surges, support the use of techniques to increase the rise time of the surges impinging on the insulation system terminations as, e.g. filters [40], [41].

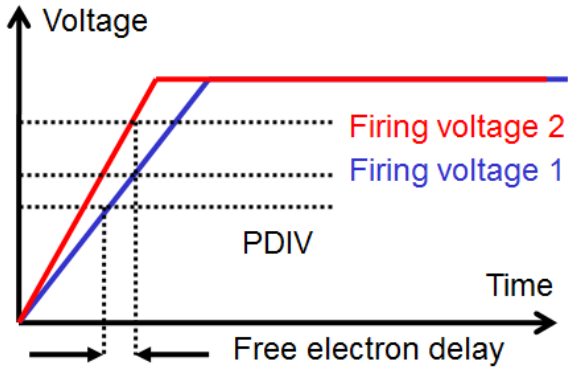

Figure 25. The effect of impulse voltage slew rate on PD magnitude.

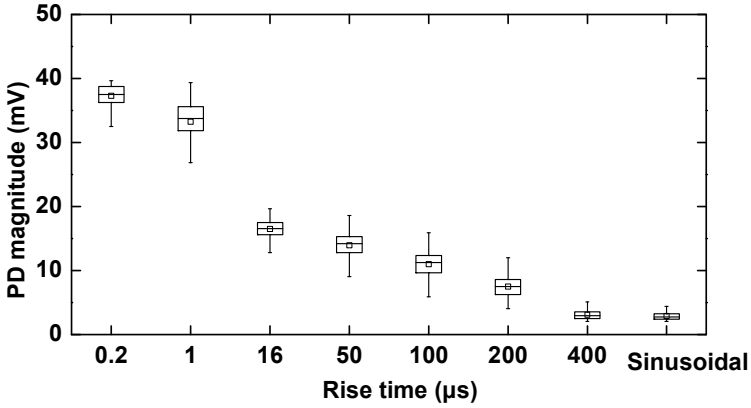

Figure 26. PD magnitude (measured in mV using an UHF detection system) as a function of voltage impulse rise time [37].

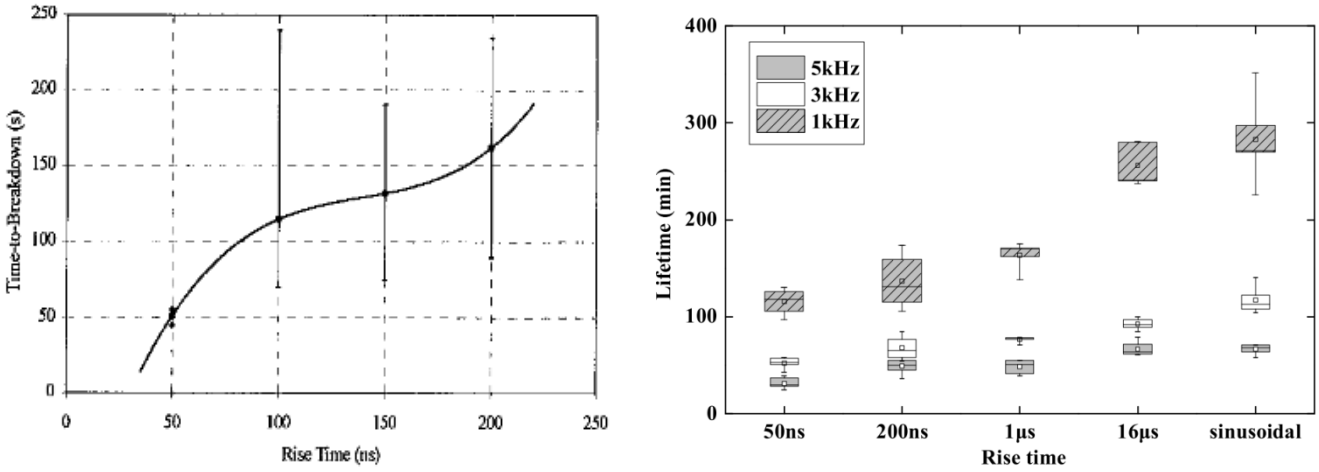

Figure 27. Lifetime of crossed enameled wires as a function of rise time (after [37] and [38]).

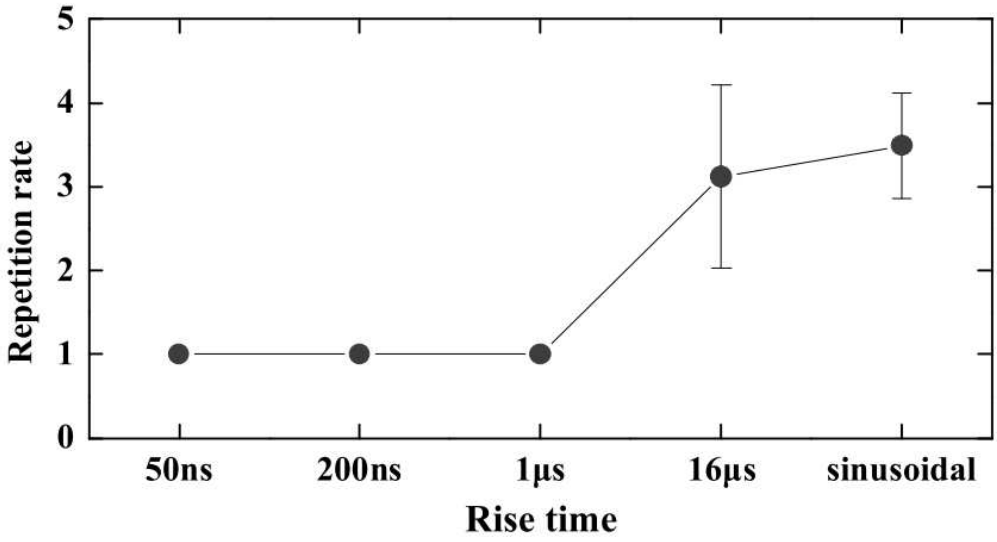

Figure 28. **PD repetition rate as a function of rise time in crossed pairs (after [37]).**

Effect of frequency

The role of frequency is not so clear as that of rise time. In general, it is possible to observe a reduction of PD magnitudes with frequency, as reported in Figure 29. Starting from this, it is clear that frequency scaling cannot be applied above RPDIV, since the interaction of PD and the dielectric could be completely different. Indeed, if one considers the average number of surges to breakdown, see Figure 30, it is possible to observe that the lowest supply frequencies tend to provide the lowest number of surges to breakdown. In other words, the degradation caused by each surge is more important when the supply frequency is low. This can be explained observing that chemical degradation in one cycle will be larget at the lowest frequencies, since the period is longer.

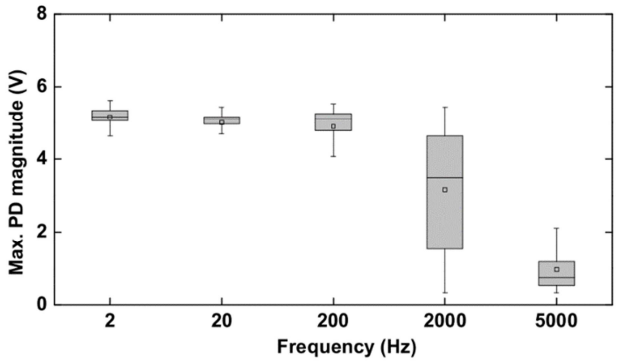

Figure 29. **PD magnitude as a function of impulse voltage frequency in crossed pairs (after [37]).**

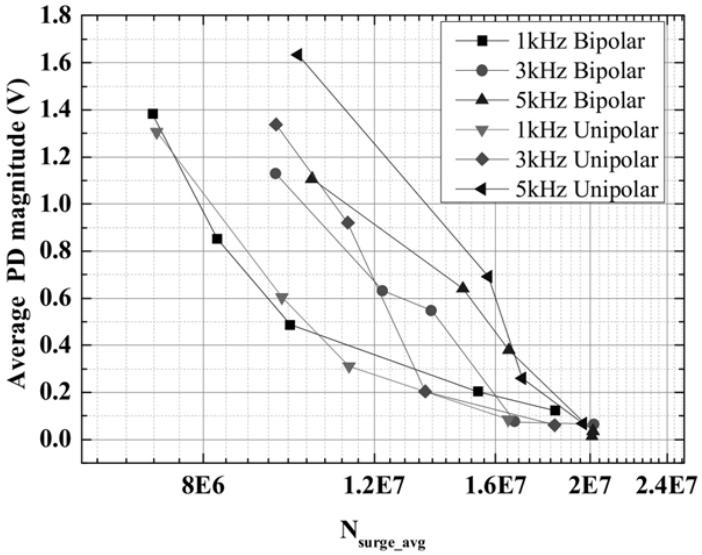

Figure 30. **PD magnitude as a function of impulse voltage frequency in crossed pairs (after [38]).**

Treeing inception

Most of the data reported above come from test on twisted pairs (i.e., magnet wires twisted together), an insulation model used to represent the turn insulation of low voltage motors. Since the wires have insulation thickness around 30 μm, the PD process occurs on the insulation surface. However, for epoxy-mica insulated machines, alternatives routes to failure are possible. One of these is the inception of trees from protrusions.

The inception of electrical trees is explained considering the damage induced by the injection/extraction of hot electrons from the polymer matrix. The process requires very high fields and can be incepted only at insulation defects, where the field is greatly enhanced with respect to the service field. As an example, the process initiates around 400-600 kV/mm in PE (under AC waveform). The hot electron injection/extraction mechanism supports a significant influence of the voltage waveform as, indeed, proved by a few references.

In [29], epoxy (Emerson and Cumming Stycast 1264 bisphenol epoxy) insulation was tested through a point-plane electrode system (needle radius: 5 μm, electrode separation 100 μm) till breakdown. For these tests, voltage pulses of variable magnitude and repetition rate were employed (voltages: 8-13 kV, frequencies: 5, 100, 5000 Hz, unipolar (pos/neg) voltage source, rise time: 500 ns, fall time: 500 ns, width: 1 μs). The results can be condensed through Figure 31, which shows the lifetimes obtained during the investigation. The authors summarize their main findings as follows:

- As the applied surge voltage increases, the life decreases following an inverse power law.
- As the repetition rate increases, the number of surges to initiate a tree increases.
- The life is shorter with positive surges than with negative surges; this contrasts with the observation that there is more electro-luminescence (EL) emitted with negative surges.
- There are significant interactions between the voltage magnitude, polarity and repetition rates, which tend to lead to a longer life than in the absence of interactions.
- If EL is not detected, then failure does not occur; if EL is detected, then failure will eventually occur.

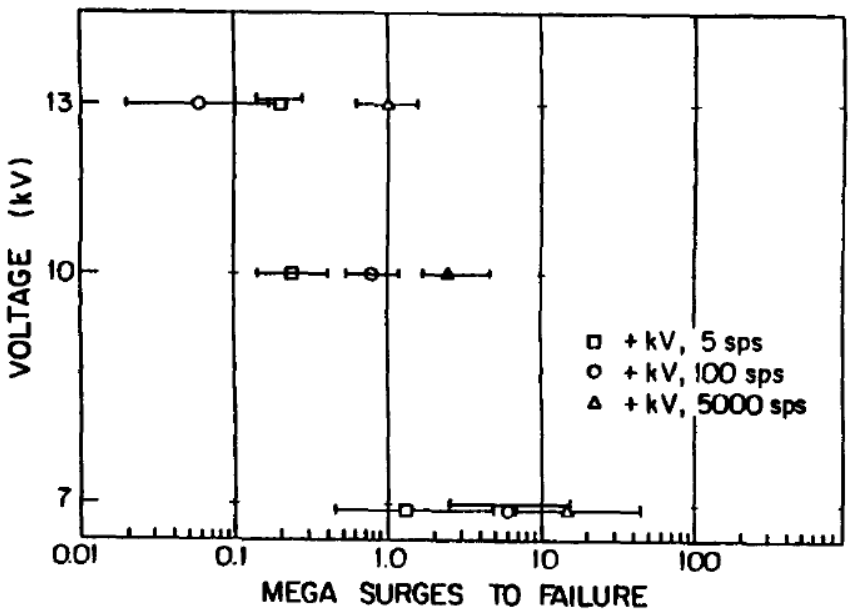

Figure 31. **Number of pulses to failure versus positive voltage at 3 different repetition rates. Horizontal bars represent 90% confidence intervals. sps – surges per second [29].**

The work was performed on a transparent epoxy: further studies are required to establish whether the results are valid for filled epoxies used in power equipment.

A similar investigation was performed by K. Nelson [30], leading a) to observe a dependence on pulse width (longer pulse give shorter lives, b) to state that dependence on frequency is scarce (contrarily to [29]. However, voltage impulse frequency and rise time (max 1 kHz, 5 μs) were different than in [29].

Space charge

As shown in Figure 9 and Figure 10, both line-to-line and line-to-ground voltages are bipolar. Space charge can be injected in these insulation system only at low frequencies when the voltage impulses have the same polarity for a time that is long enough (this might happen, e.g., in rotor-wound machines used in wind turbines, when the rotor speed approaches the synchronoization speed). Figure 32 shows experimental results that confirm that space charge accumulation can be neglected for frequencies above 50 Hz. In general, however, the influence of space charge (if any) should be neglected when compared with other effects, as PD attack.

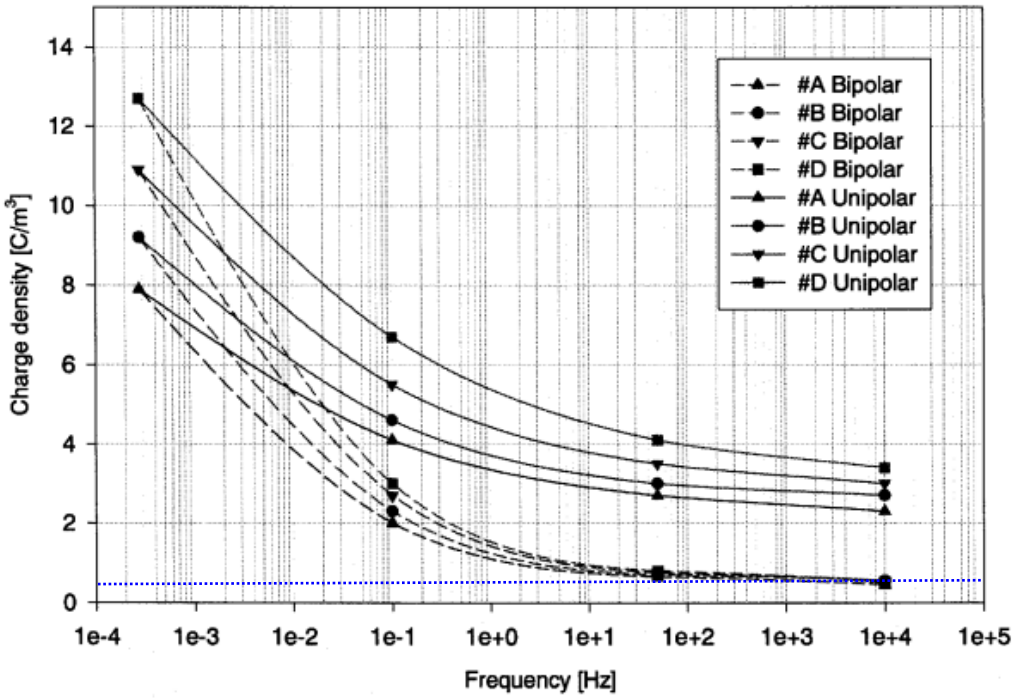

Figure 32. **Total space charge accumulated in enameled wires as a function of frequency and for both unipolar and bipolar voltage waveforms (after 1 hour of prestressing). Applied peak-to-peak voltage: 1 kV. Insulation thickness: 35 μm. The dotted line marks the instrument bias and should be considered the 0 charge level.**

Multifactor aging

Solid insulation aging solely caused by repetitive transients was a subject of investigation in the late nineties of the last century, and the dependency on material type, temperature, pollution and other effects was included.

An important issue is the occurrence of several electrical aging factors at the same time. It was earlier mentioned that aging under very fast transients not just depends on the simple parameters like voltage peak and frequency, but that the risk of failures might increase considerable in case of combined exposure. This could be combined voltages AC fundamental plus harmonics, AC plus transient, DC plustransient or any combination of these.

Fabiani et. al. [19] has presented a model which gives the possibility to combine these factors. Based on several kinds of insulation, time to failure is related to different components of the applied voltage through:

$$L = lnL_0 + a \cdot lnK_s + n \cdot lnK_p + c \cdot lnK_{rms} \tag{11}$$

where:

$$K_s = \frac{\omega_1}{\omega_0}\sqrt{\sum_{h=1}^{N} h^2 a_h^2} \tag{12}$$

$$K_p = \frac{V_p}{V_{1p}^*} \tag{13}$$

$$K_{rms} = \frac{V_{rms}}{V^*_{1rms}} \tag{14}$$

with:

- V^*_{1rms} and V^*_{1P} rms and peak value of the reference 50 Hz voltage,
- $\omega_0 = 2\pi f$ rad s^{-1}, with f equal to 50 or 60Hz.
- *h* harmonic order ($h=\omega/\omega_1$),
- $\omega_1$the angular frequency of the fundamental,
- $\alpha_h=V_h/V_1$,

N the number of harmonic components in the waveform,

P, *s* and *rms* subscripts indicate peak, shape and rms related indicators.

Considering as prevailing factor V_p, eq. (11) becomes:

$$L = lnL_0 + n \cdot lnK_p \tag{12}$$

where n is the Voltage Endurance Coefficient (VEC).

The measured time to failure is illustrated in Figure 33 including values of the voltage endurance coefficient (VEC) of the life line model coming from eq. (12). It shows significant difference between presence and absence of PD and high-frequency components with respect to the life time of insulation system very well consistent with the discussion earlier about PD and aging.

These results are not directly related to the aspect of transient exposure of solid insulation, but they clearly indicate the necessity of taking into account combined voltage applications including combinations of power frequency plus transient exposure, in this case of course mainly with focus on the very fast transients.

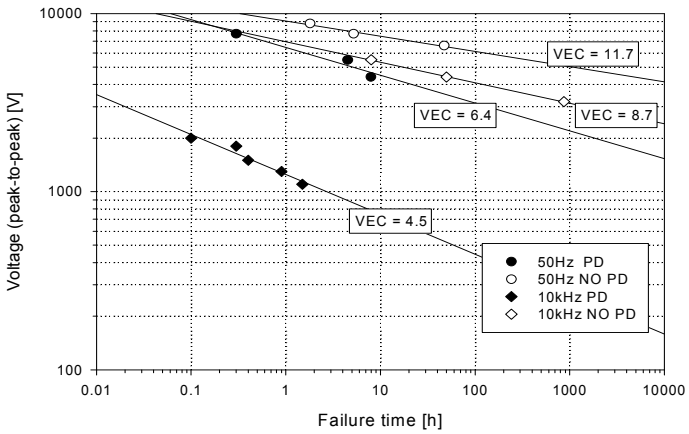

Figure 33. **Life test results under 10 kHz sinusoidal waveform for twisted pairs aged below and above the threshold for inception of partial discharges** [14].

APPARATUS-SPECIFIC ISSUES

Rotating machines

IEC 60034-18-41 [5] and 60034-18-42 [6] standards separate the systems into those which are **not** expected to experience partial discharge activity within specified conditions in their service lives (Type I) and those which **are** expected to withstand partial discharge activity in any part of the insulation system throughout their service lives (Type II).

For both Type I and Type II insulation systems, the drive system integrator (the person responsible for co-ordinating the electrical performance of the entire drive system) should inform the machine manufacturer what voltage will appear at the machine terminals in service. The machine manufacturer will then decide upon the severity of the stress levels, appropriate tests for qualifying the insulation system. The manufacturer will also label the machine with the Impulse Voltage Insulation Class IVIC, i.e., the peak to peak voltage that can be tolerated under converter operation. The severity is based on the impulse rise time, the peak to peak voltage and, in the case of Type II systems, the impulse repetition rate. After installation of the converter/machine system, it is recommended that the drive system integrator measures the phase/phase and phase/ground voltages between the terminals and ground to check for compliance.

Type I insulation system

Type I system, which are **not** expected to experience PD activity in their service lives (thus, PDIV should be larger than the operating voltages), are generally wire-wound system where the overcoat is made of an organic dielectric and does not include inorganic fillers. Equipment where Type I insulation systems are subjected to converter surges are low voltage induction motors in industrial drives, but also wind turbine stators (when back-to-back AC/AC converters are used) or, sometimes, wire-wound rotors.

Type I systems, see Figure 34, are generally realized coating wires with polyester (PE) or polyamide-imide (PAI) enamels. Aramid paper sheets are used as slot liners and for interphase separation. Since both PE and PAI are purely organic they cannot withstand PD activity for long times. In fact, electrons generated in PD avalanches can have energies in excess with respect to those of C-C and C-H bonds (7-8 eV), and Dissociative Electron Attachment [42]. processes can take place leading to radical formation and, thus, to an irreversible degradation of the polymer. Therefore, turn insulation or phase/phase insulation if Aramid paper sheets are not properly placed are bound to fail in very short times if the applied voltage is above the PD inception voltage.

For the above reasons, [5] considers that an insulation system is qualified for operation under inverter surges if PD cannot be incepted at any time of operation for a sufficiently long time.

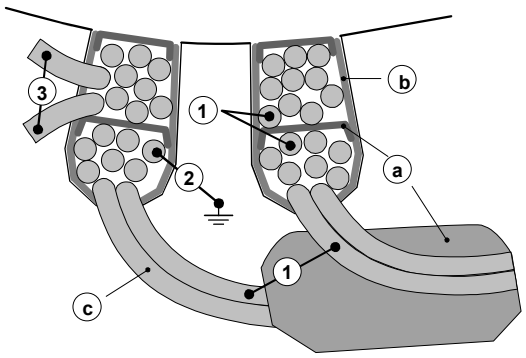

Figure 34. **Type I insulation system: a) phase insulation/endwinding insulation, b) ground insulation, c) turn insulation [5]**

Table 2 ranks the most critical factor of the voltage characteristics for the turn/turn, phase/ground and phase/phase insulation separately. The factors are weighted against their likelihood of giving rise to PD in the specified sub-system, not against their harmfulness. As an example, for the turn insulation system, the larger the jump voltage, the larger will be the interturn voltage. Furthermore, the shorter the rise time, the more uneven will be the turn voltage distribution. Both features are thus of major importance. On the contrary, the impulse voltage repetition rate, is not deemed as important, as it will not affect PD inception (although the larger the repetition rate, the faster the degradation of the turn insulation above PDIV).

Table 2. Influence of features of the machine terminal voltage on components of Type I insulation systems [5]

Insulation component	Fundamental frequency	Impulse voltage repetition rate	Peak/peak impulse voltage (Fundamental frequency)	Peak/peak impulse voltage (Impulse frequency)	Jump voltage	Impulse rise time
Turn to turn insulation	○	○	○	○	●	●
Main wall insulation	○	○	●	●	○	○
Phase/phase insulation	○	○	●	●	○	○
Note: ○ Less significant ● More significant						

IEC 60034-18-41 [5] contains a detailed series of qualification and quality control tests to ensure a PD-free motor. These are an extension of the procedures reported in [42]. However, the failure criterion is not the breakdown of the sample as in [42] but the inception of PD within the sample itself.

Type II insulation system

In Type 2 insulation systems, see Figure 35, the ground wall and phase-to-phase insulation materials are generally based on combinations of organic (epoxy, often polyester in older designs) and inorganic (mica) materials. Silicon and oxygen in the mica are connected by strong energy bonds (103.4 eV), which makes difficult for PD to cause degradation through bond-breaking processes [42]. For these reasons, in Type II electrical machines PD are generally tolerated, provided that they are not too large. However, problems may stem from turn/turn PD, as the thickness of this part of the insulation system is much lower than that of the groundwall, and sometimes realized using organic materials.

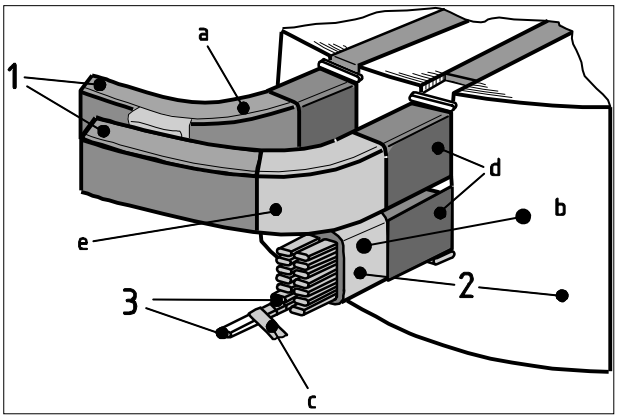

Figure 35. **Type II insulation system: a) phase insulation/endwinding insulation, b) ground insulation, c) turn insulation, d)slot corona protection, e) stress grading**

Reference [8] gives a clear overview on how different parts of rotating machine insulation will be affected by different types of voltages, as shown in Table 3. It is possible to note here that, compared with Type I insulation systems, here repetition frequency becomes one of the key factors, as PDIV can be lower than the operating voltage, thus degradation through PD inception is acceptable provided that it does not become too fast.

Table 3. Different voltage types affecting insulation components in rotating machines with type 2 insulation systems [8]

Insulation component	Fundamental frequency	Impulse repetition rate	Fundamental frequency pk/pk voltage	Jump voltage	Impulse repetition rate pk/pk voltage $U'_{pk/pk}$	Impulse rise time
Turn to turn insulation	○	●	○	●	○	●
Main wall and phase/phase insulation	●	○	●	○	○	○
Corona protection layer+ stress grading	○	●	●	●	●	●
Note: ○ Less significant ● More significant						

For Type 2 rotating machines, two main components should be carefully designed. The ground wall should be able to resist power frequency voltages and transients under PD activity. The turn-to-turn insulation should be able to resist transients, but not necessarily PD (which might not been incepted) [44]. Therefore, [8] supports voltage endurance testing as in [47][48][49]. The combination of the magnitude of the voltage overshoot, U_b, the slew rate of the voltage and its repetition frequency (f_{rep}) plays a major role in the occurrence of breakdown in rotating machines. However, the synergies between these parameters are not easy to quantify. Therefore, [8] supports the frequency acceleration rule to extrapolate test results to the operating frequency, and the inverse power law to evaluate the lifetime at the rated voltage of the machine.

Besides electrical stress, surges may also increase thermal stress which acts synergically with the electrical stress. Tests on the groundwall insulation of coils are reported in [35]. The results indicate that, in inverter-fed motors, hot spots can develop in the groundwall insulation. An average increase of ~10 °C in temperature was observed increasing the switching frequency of ~1 kHz. The results of accelerated degradation tests, reported

in Table 4, demonstrate that pulse aging is much more severe when compared with the power frequency (50/60-Hz AC) aging. In order to quantify the synergy between electrical stress and dielectric heating, tests were performed at room temperature and by using a cooling system. The drop in the service life of the groundwall insulation, with reference to the switching frequency characteristic of the power source, was ~58% in the first case, ~31% in the second case. This variation highlights the role played by dielectric heating. Insulation delaminations thus dominate the aging process under pulse applications due to high thermal and electrical stresses. The synergic effect of different stresses (Electrical, Thermal and Mechanical) is confirmed in [50].

Table 4. Lifetimes of form wound coils as a function of impulse repetition frequency, electric stress and temperature [35].

Temperature (°C)	Log (E) Stress in kV/mm	Time-to-failure Log (D) in hrs*			
		AC (Hz)	Pulse Switching Frequency (Hz)		
		60	500	1500	3000
20	1.12	2.66	2.56	2.45	2.28
	1.21	2.39	2.26	2.16	1.98
	1.29	1.98	1.85	1.76	1.65
120	1.12	2.46	2.31	2.22	2.05
	1.21	2.13	2.02	1.89	1.76
	1.29	1.83	1.76	1.51	1.45
155	1.12	2.42	2.29	2.16	2.03
	1.21	2.02	1.92	1.84	1.66
	1.29	1.72	1.59	1.49	1.38

*Average of three samples per test condition.

For stators operating above 700 volts, there may be slot corona protection present, a semiconductive coating (made out through semiconductive paints or tapes) that provides a grounded screen to the insulated stator winding in contact with the slot wall. The slot corona protection extends a few centimeters out of the stator. At this specific point, the surface of the insulation is subject to a stress concentration which could be large enough to incept PD. Therefore, for high voltage machines, a stress grading system is generally used.

High frequency voltage pulses are known to cause an accelerated degradation of stress grading systems. The fast leading edges and high repetition rate of the voltage pulses lead to an increased electric and thermal stress on stress grading (SG) coating used to control the electric field in stator end windings [51][53]. Even if the SG coating is designed to keep the electric field below the surface discharge level, this capability will be necessarily accompanied by increased heat generation in the coating. Degradation [54] and loss of resistivity and nonlinearity of the SG material [55] can be consequences of an increased temperature that in some cases can reach 55 °C above the surrounding area that observed under sinusoidal 50/60 Hz frequency [56]. As a consequence, not only the electric field must be controlled but also the ohmic heat generation that has been identified as a potential problem in SG coatings of motors fed by fast repetitive pulses [55] [56].

In order to ensure a satisfactory lifetime for the SG system, appropriated design procedures have to be devised to ensure that the maximum hot spot temperature at the stress grading coating surface will not raise above the assigned temperature limit at the maximum expected operating temperature of the machine [57].

In addition, simulations of the stress-grading systems using finite element analysis verified by experimental results [58][59][60], indicate that, during the fast rise-time, a high electric stress can develop right at the slot exit of the stator if the conductivity of the slot corona protection coating is not high enough (see *Figure 36*). During the rise-time,

the stress-grading coating is not performing its intended function. After the rise-time of the pulses, the stress shifts to the SG coating, and the grading of the electric stress becomes effective. This phenomenon appears because of the relatively low conductivity of the slot corona protection coating during these fast pulses. Increasing the conductivity of the slot corona protection coating alleviates the problem, but it increases the eddy current loss in the stator laminations. In addition, it can be mentioned that other impulse voltages caused e.g. by switching impulses are most significant for ground and phase-to-phase insulation.

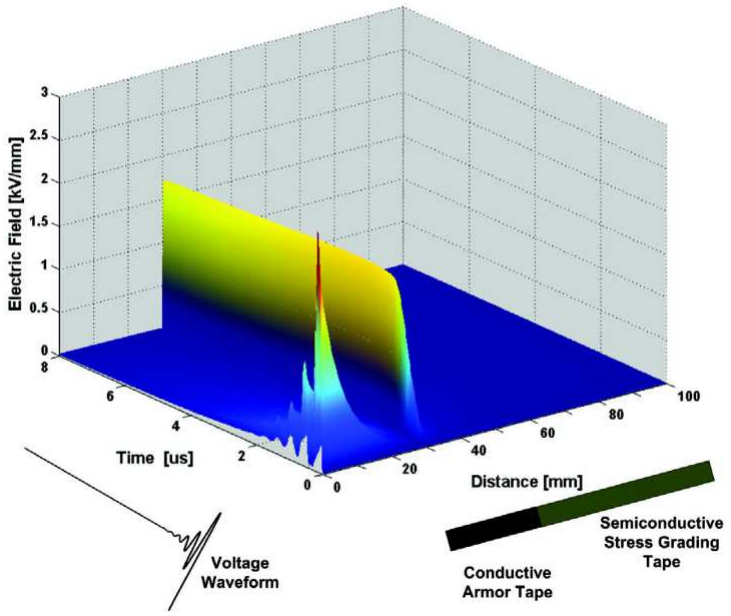

Figure 36. **Electric field grading along a grading system as a function of the voltage waveform rise time [59].**

Transformers

The effect of square voltage waveforms on transformer insulation materials has not been discussed extensively. Some tests were performed in the lab on kraft paper layers having a thickness of 60 μm and embedded between Rogowski electrodes [61]. In particular, test were conducted by increasing the applied voltage in ramps of 1 kV/min. The results, reported in Figure 37, show that the PDIV has a remarkble dependence on the surge repetition rate (frequency) and, to a lesser extent on the surge rise time. Since surge trains with the higher frequency componets favor PD inception, it could be speculated that dielectric losses are large enough to favor the formation of gas bubbles within the paper. Figure 38 shows a similar dependence on surge repetition rate and rise time for breakdown voltage. These results highlight that PWM waveform could be an issue in paper/oil transformers as well.

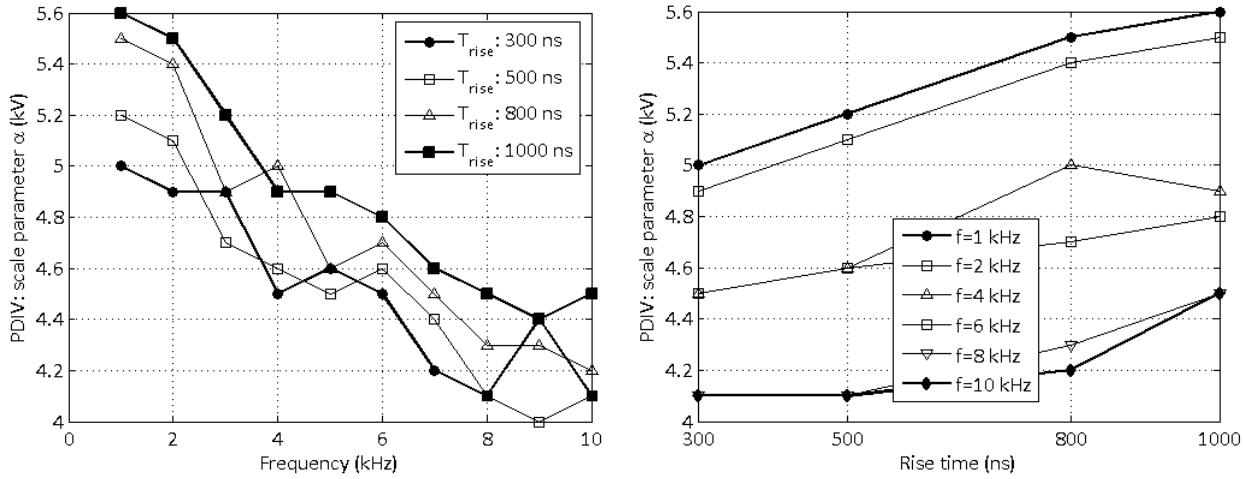

Figure 37. **Partial discharge inception voltage (PDIV) of kraft paper sheet as a function of voltage impulse rise time (T_{rise}) and repetition rate (f) [61].**

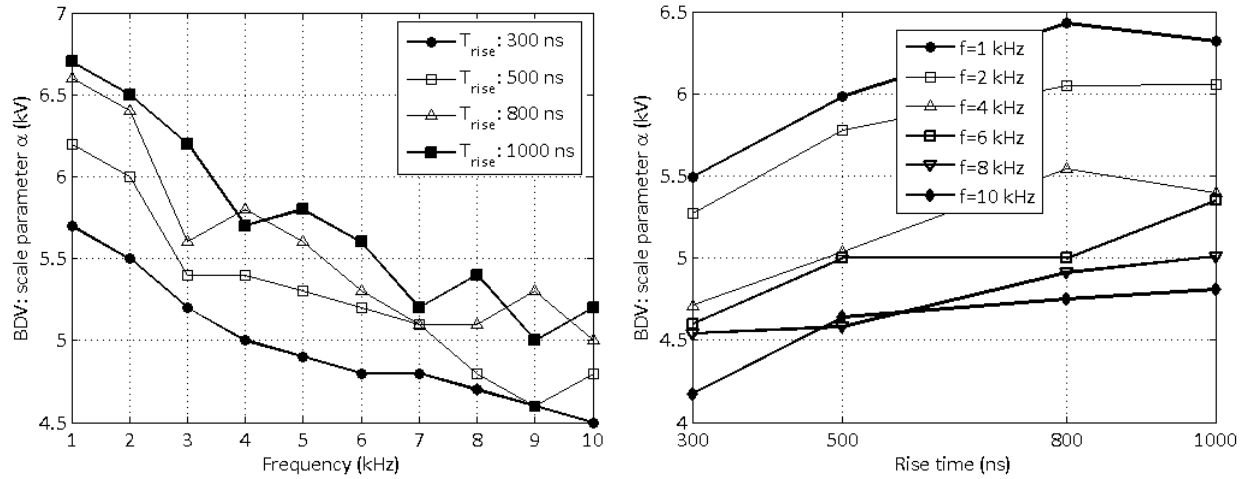

Figure 38. **Breakdown voltage of kraft paper sheet as a function of voltage impulse rise time (T_{rise}) and repetition rate (f) [61].**

For transformers, it is well known that they exhibit a complex response characteristic versus frequency which to some degree can be compared to the transient behaviour of rotating machines [62][63]. However, the construction of transformers however, tackles uneven voltage distribution under transients through additional layers of insulation at selected places of the transformer windings, disk design and conductor connections. In addition, field control by means of metallic shields can improve the insulation resistance against transients. Therefore, the impact of repetitive voltage surges can be dealt with at the design level, provided that the converter/transmission line/transformer interactions have been specified correctly.

A specific issue related to transformers is the presence of internal resonances which will interact with the circuits connected to the transformer. Figure 39 provides an example of the frequency dependency of the admittance between different transformer couplings, measured at a low voltage level. It is obvious that there is a considerable risk of repetitive transients to interact with some of these resonances and the insulation endurance must match this exposure.

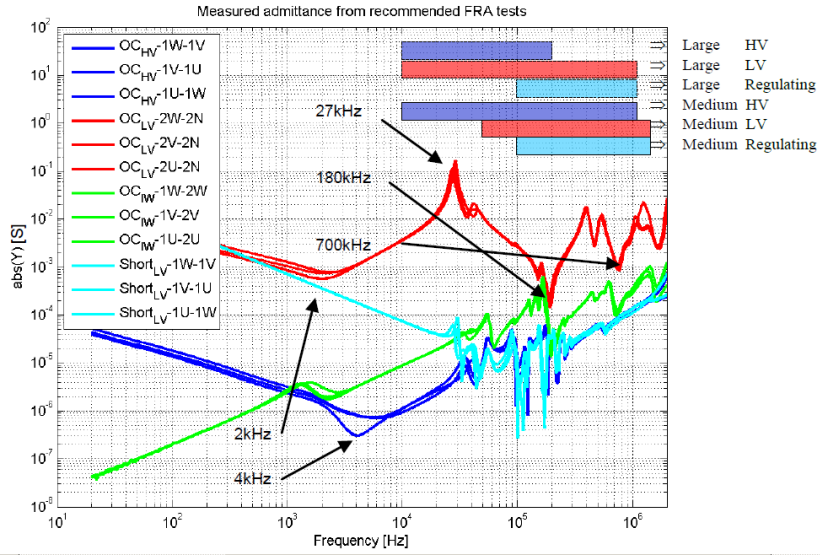

Figure 39. **Measured admittance on 100kVA dry type transformer. The diagram shows responses between different windings [63].**

Cables

For cables, it is well known that PE-based polymers and EPR do not show remarkable changes in the complex permittivity within the range of frequencies covered by converter surges [63]. Therefore, the most critical point is the termination, where surges could double their magnitude and their frequency content may impact on resistive grading system. Similarly to what happens in rotating machines, electrical field enhancement causes the hot-spot on the non-geometric cable termination (i.e., termination made of non-linear stress grading material). Similarly to SG systems in rotating machines, hot-spot are generally in the overlap area, i.e. where the semi-conductive layer on top of the insulation ends and interfaces with stress grading layer of the termination. The rise in the surface temperature of the hot-spot region is mainly due to the power loss as a result of ohmic losses at the overlap of semi-conductive screen end and stress grading layer. The power loss is the reason for temperature rise under high frequency stress. Patel et alia [64] reported hot spots up to 9-10°C (Figure 40).

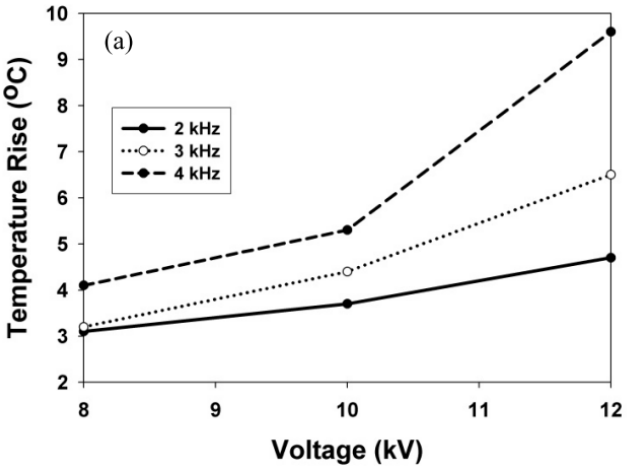

Figure 40. **Measured hot spot temperature on resistive grading systems of cable termination subjected to repetitive voltage impulses of different frequencies and magnitudes**

Finally, since water tree growth time shows correlation with the number of zero crossings of the voltage waveform, surge trains with high repetition rates lead to accelerated water tree growth [65].

TESTING COMPONENTS WITH IMPULSE VOLTAGES

Testing of components with respect to their resistance to repetitive pulses requires a) definition of pulses and procedures to be applied and b) a test setup representing the material or the equipment to be tested, c) a suitable test generator. To date, standardization of testing techniques has been developed extensively for rotating machines only. For this reason, reference will be made to rotating machines having insulation systems of both Type I and II..

It is important to notice that testing can be performed in order to assess that:

a) PD are not incepted within the insulation system throughout its entire life provided that the applied electrical stress does not exceed some prescribed values or, alternatively,
b) the system is able to withstand the electrical stress (possibly combined with other stresses) long enough to ensure the reliability of the system.

As observed before, (a) applies to purely organic insulation systems, (b) to mixed organic/inorganic systems.

Also, it important to distinguish between

- **qualification tests**, aimed at proving the reliability of the insulation (thus involving accelerated life test on a statistically meaningful number of specimens) and,
- **type tests**, performed on a complete equipment.

For economical reasons, qualification tests cannot be performed on complete equipment and insulation models need to be used. In the following section, the models typically used to

Insulation models

Twisted pairs

Twisted pairs are used to qualify turn/turn insulation systems in wire wound machines. Twisted pairs consist of a couple of magnet wires twistet together. If the final manufacturing of the motors involves further treatments, e.g. dipping and baking, twisted pairs should undergo the same processes of the stator. The ASTM D1676-03 standard requires that samples are realized with 30 twists with a length of 120 mm inches for the twisted area [67], [68].

Figure 41. **Twisted pair**

Motorettes

Motorettes (see Figure 42) simulate all parts of the insulation system, i.e., the turn/turn, phase/ground and phase/phase of a random wound machine. Motorettes are made placing two coils in contact (with an Aramid paper layer as a separator when phase/phase insulation system need to be simulated). These coils are assembled within L-shaped aluminum parts simulating the slots. If the machine is varnished, or dipped in epoxy resin and baked, the motorette should undergo the same process [42].

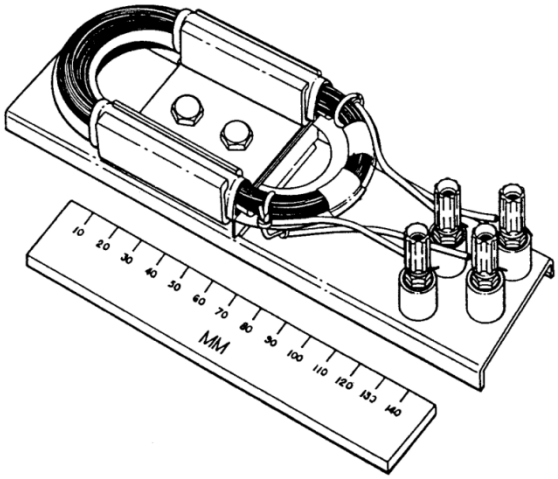

Figure 42. **Motorette [42]**

Formettes/statorettes

Formettes are used to qualify the mainwall insulation and stress control system to be used in the stator of Type II system (or form wound Type I machine, e.g. hairpin machines). Formettes are coils built to production standards and fitted into representative slots.

Formettes should be made to the full manufacturing specification for a production machine. They should represent, as accurately as possible, the characteristics of a full-size motor or generator, including, but not limited to, size, construction (including tying, bracing, and blocking), geometry (curved or circular rather than flat), and interfaces (coil and lead connections). The slot length may be reduced to minimize the capacitive load. Examples of formettes are shown in Fig. 43. Alternatively, statorettes (see Fig. 44) can be used for small size machines.

Figure 43. **Formette [50]**

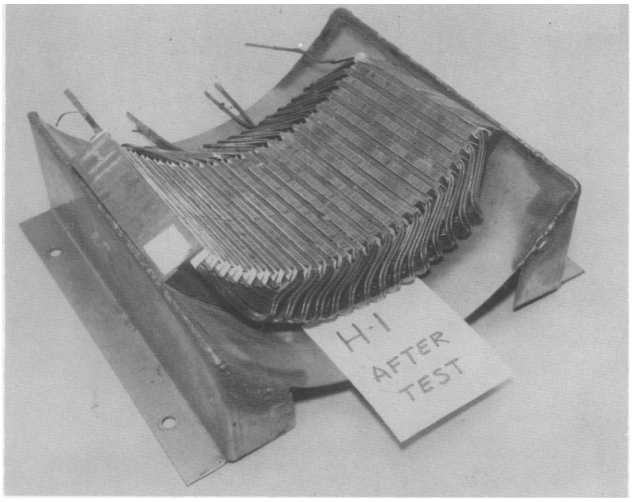

Figure 44. **Statorette [51]**

Turn/turn samples

Turn/turn samples are the equivalent of twisted pair for of Type II system (or form wound Type I machine, e.g. hairpin machines). These samples should represent the insulation system used in machines in terms of materials and dimensions. Pairs of insulated conductors are held together with the terminals splayed apart and processed according to production standards. The insulated conductors should be in contact along the length of the straight portion to simulate the contact between turns in a coil. To maintain this contact it may be necessary to process the samples using pressing operations and/or VPI, as required by the design and materials.

Compared with twisted pairs, two main differences exist. The first is that fillers (indicated by (4) in Fig. 44) are needed to prevent the inception of PD in the air wedges where the two insulated conductors separate one from the other. The second is related to the impregnation procedure. Impregnation using the VPI technique is often too good for these small size samples. As a result, cavities within the insulation of these models are generally much smaller than those observed in the insulation system of the machine. For these reasons, it appears that the IEC will support the use of formettes or formettes even for turn/turn insulation testing.

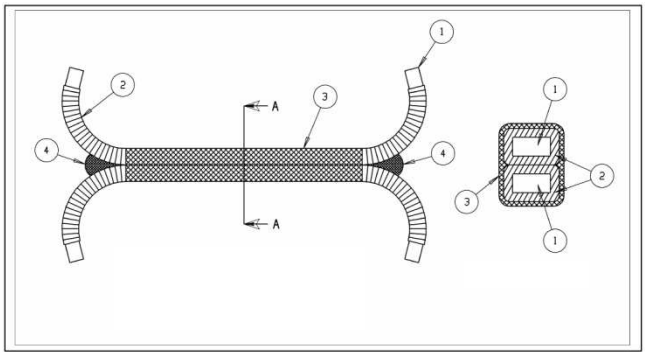

Key
1. Copper conductor
2. Turn insulation
3. Mainwall insulation overlaid with protective glass armour tape
4. Non-conductive, one-part silicone filler (or equivalent)

Figure 45. **Turn/turn sample [6]**

Rotating machines testing

Stress categories

The voltage applied to the machine terminals depends on the inverter DC bus voltage, on the cable/winding reflection coefficient (which in turn depends on the rise time of the surge, on the cable length and on the cable and winding surge impedances). These quantities determine the characteristics of the phase/phase and phase/ground voltages. Furthermore, the maximum voltage applied to the turn insulation depends on the peak of the jump voltage multiplied by a coeffient, α, that will depend on the rise time of the voltage waveform as well as on the geometry and electrical characteristics of the winding. As calculations to derive this coefficient are not straightforward, worst case estimates are provided in [5] (see Figure 13).

From the above, it comes out that two features of the appllied voltage surge will affect the insulation, i.e. the overshoot factor (OF) providing the ratio between the DC bus voltage and the peak voltage at machine terminals, and the rise time. The severity of the stress will increase for increasing OF values and decreasing rise times. The IEC has standardized this concept into the so-called **Stress categories**, which are synthetized in Table 5.

Table 5. Stress categories

Stress category	Overshoot factor (OF) U_p/U_{dc}	Impulse risetime t_r (µs)
A – Benign	**OF** $\leq 1{,}1$	0,2 ± 0,1
B – Moderate	$1{,}1 <$ **OF** $\leq 1{,}5$	
C - Severe	$1{,}5 <$ **OF** $\leq 2{,}0$	
D - Extreme	$2{,}0 <$ **OF** $\leq 2{,}5$	

It is important to stress that, the stress category of an insulation system is qualified for (let us assume it is C, as an example) will be printed on the plate as: IRV C, where IRV means **Impulse Rated Voltage**.

Type I insulation system

Type I insulation system are **not** expected to experience PD activity during their service lives. Both qualification and type tests should therefore ensure that the system is always working below the PDIV. Therefore, PD measurements are carried out at regular times during the aging procedure to ensure that the system is PD free up to some specified voltage level.

Qualification tests are performed to investigate the capability of the winding insulation to withstand various stresses. PDIV measurements are carried out before and after thermal cycling and other tests as defined in [43], as well as voltage stressing at one of the stress category levels enhanced by a safety factor. The peak value of the test voltage, U_{peak}, is thus calculated starting from the DC bus voltage of the inverter, U_{dc}, as:

$$U_{peak} = U_{dc} \cdot OF \cdot \mathrm{K} \cdot \mathrm{EF} \tag{13}$$

Where K and EF are explained below:

- K is the insulation system factor, i.e., a factor which models (based on empirical evidence and worst case criteria) the propagation of the peak voltage inside across the insulation sub-systems. In particular:

- Phase/Phase insulation sub-system: K = 1
- Phase/Ground insulation sub-system: K = 0.7
- Turn/Turn insulation sub-system: K = 0.7

- EF stands for Enhancement Factor, it is the safety factor. The EF value were decided by the IEC Technical Committee based on empirical considerations. The standard provides EF value ranges which depend on the insulation sub-system. As an example, the following values can be selected:
  - Phase/Phase insulation sub-system: EF = 1.63
  - Phase/Ground insulation sub-system: EF = 1.38
  - Turn/Turn insulation sub-system: EF = 1.63

The test levels obtained through the standard procedure are suitable for qualification purposes. For type testing of the insulation, the same levels should be increased by a factor equal to 20%, since type test do not include the effect of aging.

As mentioned above, the test samples are to be made using the materials and manufacturing routes applicable for production. In general samples can represent part of the insulation system or insulation system in total. Since insulation models are not affected by the uneven distribution of the turn voltage typical of complete windings, sinusoidal voltages can be used extensively when testing the turn/turn insulation in motorettes or even (if a special winding is used) complete windings, see Table 6.

Table 6. Allowed voltage waveforms

Component to be tested	Design qualification tests				Type test	
	Twisted pair or equivalent		Motorette or complete winding		Complete winding	
	Sine	Impulse	Sine	Impulse	Sine	Impulse
Turn/turn	✓	✓	*	✓	*	✓
Phase/phase	No	No	✓	✓	✓	✓
Phase/ground	No	No	✓	✓	✓	✓

* A special test winding is required in which the turn/turn insulation is simulated by at least two electrically isolated conductors wound in parallel, one of which is grounded and the other is energised

Type II insulation system

For Type II machines, the turn insulation is generally the weakest point Thus, the electrical life of the turn insulation must last as long as or longer than mainwall insulation. It is expected that the manufacturer will know what is the maximum peak voltage, U_{turn}, that could appear between turns in a particular service application. If not, it should be assumed that the complete jump voltage may fall across the first coil. Similarly to what shown for Type I machines, U_{turn} should be increased by a safety factor, in accordance with the manufacturer's design rules, to give the basic peak test voltage, U_{peak}.

The testing is in two stages. In the first stage, U_{peak}, is applied between the two conductors of the test sample as a 50 or 60 Hz sinusoidal voltage for 60 seconds. If PD are not incepted, it may not be necessary to perform the qualification test. Otherwise, if PD activity is detected, a voltage endurance test is to be performed. This will consist of applying repetitive impulses as described in [46] or a sinusoidal voltage having larger amplitude and repetition frequency compared with the converter. The test is terminated when electrical breakdown occurs. By increasing the voltage magnitude and frequency, the acceleration of the ageing process that leads to electrical failure is attained. This is a desirable feature of the test method. However, the inception of degradation mechanisms normally not active in service should be avoided. Techniques for accelerated voltage ageing are described in [45][46][48].

Endwinding stress grading system lifetime is influenced by two factors: applied voltage and temperature. Ideally, a test is required in which sample bars, prepared with a corona protection layer and stress grading material, are arranged in simulated slots and subjected to voltage impulses that match or exceed in severity the impulses to be withstood in service. The bars may be shorter than in the service machine in order to reduce the capacitive load on the impulse generator. However, they should replicate all other design features. The test should continue for 100 hours. It is recommended that during testing the location and intensity of "hot spots" should be evaluated using an infrared camera, and the surface PD observed by an ultraviolet sensitive camera or in a darkened room [51].

NANOCOMPOSITES

For low voltage rotating machines, one of the possible solutions to improve the insulation reliability consist of inverter surge resistant wire with nanocomposite coating [69]-[73]. Nanocompsoite enameled wires, which have excellent resistance to the PDs, were developed by Hitachi Magnet Wire Corporation [74][75]. The enameled wires are composed of inner coating with polyester-imide/silica nanocomposite and outer coating with polyamide-imide as shown in Figure 46. Insulation breakdown time of the nanocomposite enameled wire under 10kHz sinusoidal voltages is shown in Figure 47. The nanocomposite enameled wires show longer insulation breakdown time than that of the conventional enameled wires. Silica nano-fillers, in fact, exhibit much higher PD resistance with respect to pure polymer materials. Therefore, the silica nano-fillers in the coating prevent PD erosion efficiently, and the nanocomposite enameled wires show excellent resistance to the PDs compared to the conventional enameled wire. In particular, at low voltage such as 1.13kV, the nanocomposite enameled wires show more than 1,000 times longer breakdown time than that of the conventional enameled wire.

Toshiba Corporation and Unimac Ltd. also developed nanocomposite enameled wires with nano-clay dispersed coating [76][77]. Flexibility is one of the important properties for enameled wires, because they are usually used in random winding coil. To evaluate the flexibility of the wire, the crack number of the wire surface was measured when it was wound up 100 turns around itself. The nanocompsoite enameled wire had no cracks as same as the conventional enameled wire, which indicates that the nanocomposite enameled wire has sufficient flexibility. Furthermore, Figure 48-(a) compares the insulation breakdown time between the nanocomposite and conventional enameled wire under 60Hz-2kV at 150°C. The twisted pair specimen of the nanocomposite enameled wire has insulation breakdown time 16 times longer than that of the conventional enameled wire. Indeed, the nano-clays in the coating prevent PD erosion efficiently. In particular, the plate-shaped and oriented nano-clays seem to enable the nanocomposite enameled wire to have excellent resistance to PDs as shown Figure 48-(b).

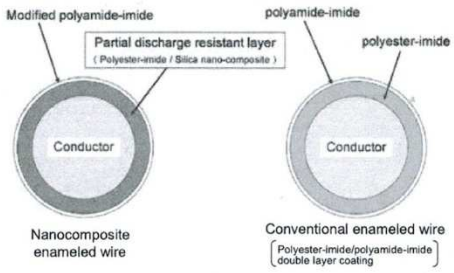

Figure 46. **Cross section structure of nanocomposite enameled wire [75].**

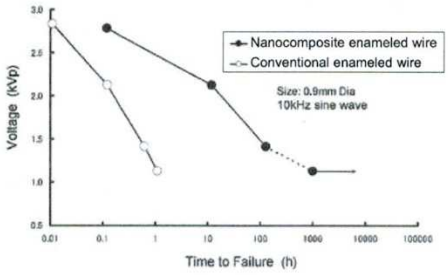

Figure 47. **Comparison of insulation breakdown time of nanocomposite and conventional enameled wires [75].**

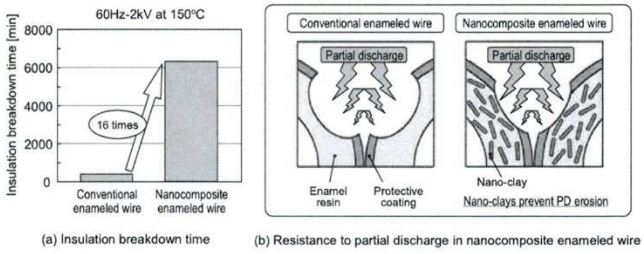

Figure 48. **Comparison of insulation breakdown time between nanocomposite and conventional enameled wires [76].**

REFERENCES

[1] IEC 60071-1:2006. Insulation co-ordination - Part 1: Definitions, principles and rules

[2] 60060:High-voltage test techniques - Part 1: General definitions and test requirements

[3] IEC 61800-8 TS Ed. 1.0, *Adjustable speed electrical power drive systems – Part 8: Specification of voltage on the power interface*, 2010.

[4] IEC 60034-25 TS Ed. 2.0, *Rotating electrical machines – Part 25: Guidance for the design and Performance of a. c. motors specifically designed for converter supply*, 2007.

[5] IEC 60034-18-41:2014 Rotating electrical machines - Part 18-41: Partial discharge free electrical insulation systems (Type I) used in rotating electrical machines fed from voltage converters - Qualification and quality control tests

[6] IEC TS 60034-18-42:2008 Rotating electrical machines - Part 18-42: Qualification and acceptance tests for partial discharge resistant electrical insulation systems (Type II) used in rotating electrical machines fed from voltage converters.

[7] Fabiani, D.; Montanari, G.C.; Cavallini, A.; Mazzanti, G., "Relation between space charge accumulation and partial discharge activity in enameled wires under PWM-like voltage waveforms," in IEEE Trans. on Dielectrics and Electrical Insulation, vol.11, no.3, pp.393-405, Jun 2004

[8] S. Moriyasu, Y. Okuyama, "Surge propagation of PWM-inverter and surge voltage on the motor", *IEEJ Trans. on Industry Applications*, Vol. 119, No. 4, pp.508-514, 1999

[9] K. Tsuji, K. Wada, H. Muto, H. Otsuka,O. Yashiro and N. Nagaoka, "Propagation of inverter surge and voltage distribution in motor winding", *IEEJ Trans. on Industry Applications*, Vol. 126, No. 6, pp.771-777, 2006.

[10] A. Mbaye, J. P. Bellomo, T. Lebey, J. M. Oraison and F. Peltier, "Electrical stresses applied to stator insulation in low-voltage induction motors fed by PWM drives", *IEE Proc. Electr. PowerAppl.,* Vol. 144, pp. 191-198, 1997.

[11] K. Hitosugi, S. Moriyasuand T.Kobaru, "Voltage distribution in the winding of PWM inverter motor", *IEEJ Trans. on Industry Applications*, Vol. 122, No. 7, pp.714-721, 2002

[12] K.Obata and R. Takeuchi, "Turn-to-turn voltage of windings in motors fed by inverter drives," in *Proceedings of the IEEE International Electric Machines and Drives Conference*, pp. 119-125, 2009.

[13] G. C. Stone, S. Campbell and S. Tetreault, “Inverter-Fed Drives: Which Motor Stators are at Risk?”, *IEEE Ind. Appl. Mag.,* Vol. 6, pp. 17-22, 2000.

[14] D. Fabiani, Accelerated degradation of ac-motor winding insulation due to voltage waveforms generated by adjustable speed drivers, Gedit (Bologna, Italy), 2003

[15] Petrarca, C.; Maffucci, A; Tucci, V.; Vitelli, M., "Analysis of the voltage distribution in a motor stator winding subjected to steep-fronted surge voltages by means of a multiconductor lossy transmission line model," IEEE Transactions on Energy Conversion, vol.19, no.1, pp.7,17, March 2004

[16] Grandi, G.; Casadei, D.; Reggiani, U., "Equivalent circuit of mush wound AC windings for high frequency analysis," Proceedings of the IEEE International Symposium on Industrial Electronics, 1997. ISIE '97., vol.1, no., pp.SS201,SS206 vol.1, 7-11 Jul 1997

[17] Mirafzal, B.; Skibinski, G.L.; Tallam, R.M.; Schlegel, D.W.; Lukaszewski, R.A, "Universal Induction Motor Model With Low-to-High Frequency-Response Characteristics," , IEEE Transactions on Industry Applications, vol.43, no.5, pp.1233,1246, Sept.-oct. 2007

[18] Suresh, G.; Toliyat, H.A; Rendusara, D.A; Enjeti, P.N., "Predicting the transient effects of PWM voltage waveform on the stator windings of random wound induction motors," IEEE Transactions on Power Electronics, vol.14, no.1, pp.23,30, Jan 1999

[19] Martinez-Tarifa, J.M.; Amaras-Duarte, H.; Sanz-Feito, J., "Frequency-Domain Model for Calculation of Voltage Distribution Through Random Wound Coils and Its Interaction With Stray Capacitances

[20] Guastavino, F.; Torello, E.; di Lorenzo del Casale, M.; Egiziano, L.; , "Voltage distortion effects on insulation systems behaviour in ASD motors," Electrical Insulation and Dielectric Phenomena, 2003. Annual Report. Conference on , vol., no., pp. 608- 611, 19-22 Oct. 2003

[21] A. Boglietti, P. Ferraris, M. Lazzari, and F. Profumo, “Energetic behavior of soft magnetic materials in the case of inverter supply,” IEEE Transactions on Industry Applications, vol. 30, pp 1580-1587, Nov/Dec 1994.

[22] Boglietti, A; Ferraris, P.; Lazzari, M.; Pastorelli, M., "Influence of the inverter characteristics on the iron losses in PWM inverter-fed induction motors," IEEE Transactions on Industry Applications, vol.32, no.5, pp.1190,1194, Sep/Oct 1996

[23] Kaufhold, M.; Borner, G.; Eberhardt, M.; Speck, J., "Failure mechanism of the interturn insulation of low voltage electric machines fed by pulse-controlled inverters," in Electrical Insulation Magazine, IEEE , vol.12, no.5, pp.9-16, Sept.-Oct. 1996

[24] G.C. Montanari. ”Power Electronics and Electrical Apparatus: a Threat?”. In: NORD-IS. Lyngby, Denmark 2007.

[25] Fabiani, D., G.C. Montanari, and A. Contin. Aging acceleration of insulating materials for electrical machine windings supplied by PWM in the presence and in the absence of partial discharges. in Solid Dielectrics, 2001. ICSD '01. Proceedings of the 2001 IEEE 7th International Conference on. 2001.

[26] Foulon, N., et al. Investigation of the failure mechanism of insulation subjected to repetitive fast voltage surges. in Electrical Insulation Conference, 1997, and Electrical Manufacturing & Coil Winding Conference. Proceedings. 1997.

[27] Sahlen, F., et al. Investigation of mica based insulation for high voltage machines subjected to repetitive pulsed voltage. in Electrical Insulation (ISEI), Conference Record of the 2010 IEEE International Symposium on. 2010.

[28] Mackersie, J.W., et al. The electrical properties of filled epoxy resin systems - a comparison. in Solid Dielectrics, 2001. ICSD '01. Proceedings of the 2001 IEEE 7th International Conference on. 2001.

[29] Stone, G.C., R.G. van Heeswijk, and R. Bartnikas, Investigation of the effect of repetitive voltage surges on epoxy insulation. Energy Conversion, IEEE Transactions on, 1992. 7(4): p. 754-760.

[30] J. K. Nelson, "The Nature of Divergent-field Surge-voltage Endurance in Epoxy Resin", IEEE Trans. on Dielectrics and Electrical Insulation, vol. 7, no. 6, pp. 764-772, December 2000.

[31] Kessler, M., C. Roggendorf, and A. Schnettler. Behavior of elastic syntactic foams under impulse voltage stress. in Electrical Insulation (ISEI), Conference Record of the 2010 IEEE International Symposium on. 2010.

[32] K. Bauer, M. Kaufhold, H. Wang, “High voltage motor winding insulation for high power adjustable speed drives fed by IGBT-converter”, *inProc. INSUCON’98*, pp. 257-263, 1998.

[33] K. Obata , K. Fukushi and R. Takeuchi, “Lifetime characteristics of electtrical insulation in motor fed by inverter”, *IEEJ Trans. on Fundamentals and Materials*, Vol. 125, No. 3, pp.261-267, 2005

[34] M. Kaufhold, K. Schaefer, K. Bauer and M. Rossmann, “Medium and high power drive systems; requirements and suitability proof for winding insulation systems”, *inProc. INSUCON’06*, pp. 86-92, 2006.

[35] S. U. Haq, S. H. Jayaram, E. A. Cherney, "Insulation Problems in Medium-Voltage Stator Coils Under Fast Repetitive Voltage Pulses", IEEE Trans. on Industry Applications, vol. 44, no. 4, pp. 1004-1012, 2008.

[36] Dao, N.L., et al. The changes in electrical properties of XL4421 insulation under repetitive lightning impulse voltages. in Electrical Insulation (ISEI), Conference Record of the 2010 IEEE International Symposium on. 2010.

[37] Peng Wang; Cavallini, A.; Montanari, G.C.; Guangning Wu, "Effect of rise time on PD pulse features under repetitive square wave voltages," in IEEE Trans. on Dielectrics and Electrical Insulation, vol.20, no.1, pp.245-254, February 2013

[38] Peng Wang; Cavallini, A.; Montanari, G., "The influence of repetitive square wave voltage parameters on enameled wire endurance," in IEEE Trans. on Dielectrics and Electrical Insulation, vol.21, no.3, pp.1276-1284, June 2014

[39] S. Grzybowski and N. Kota, ‘‘Lifetime characteristics of magnet wires under multistress conditions’’, in *Proc. IEEE CEIDP ’05*, pp. 605-608, 2005.

[40] P.T. Finlayson, “Output Filters for PWM Drives with Induction Motors”, *IEEE Industry Application Magazine*, Vol. 4, No.1, pp. 46-52 , 1998.

[41] T. Shimizu, M. Saito, M. Nakamura and N. Tanaka, “Analysis of motor surge voltage under the use of a surge suppression cable”, *IEEJ Trans. on Industry Applications*, Vol. 129, No. 9, pp.914-921, 2009.

[42] Sanche, Leon, "Nanoscopic aspects of electronic aging in dielectrics," in Dielectrics and Electrical Insulation, IEEE Transactions on , vol.4, no.5, pp.507-543, Oct 1997

[43] 60034-18-21 Ed.2: Rotating electrical machines - Part 18-21: Functional evaluation of insulation systems - Test procedures for wire-wound windings - Thermal evaluation and classification

[44] M. K. W. Stranges, G. C. Stone, and D. L. Bogh, “Voltage Endurance Testing Stator Insulation Systems for Inverter-fed Machines”, IEEE Industry Application Magazine, Vol.15, No.6, pp. 12-18, 2009.

[45] IEC TS 61251:2008, Electrical insulating materials - A.C. voltage endurance evaluation - Introduction

[46] IEC 62068:2013 Electrical insulating materials and systems - General method of evaluation of electrical endurance under repetitive voltage impulses

[47] 60034-18-31 Ed.2: Rotating electrical machines – Part 18-31: Functional evaluation of insulation systems - Test procedures for form-wound windings – Thermal evaluation and classification of insulation systems used in rotating machines

[48] IEC 60034-18-32 Ed. 2.0, Rotating electrical machines – Part 18-32: Functional evaluation of insulation systems – Test procedures for form-wound windings – Evaluatioon by electrical endurance, 2010.

[49] IEEE Std. 522, *Guide for Testing Turn Insulation of Form-Wound Stator Coils for Alternating-Current Electrical Machines*, 2004.

[50] Chen, W.; Gao, G., "Using multi-stress aging test to evaluate and improve medium-voltage stator insulation for adjustable speed drive applications," in Petroleum and Chemical Industry Conference (PCIC), 2011 Record of Conference Papers Industry Applications Society 58th Annual IEEE , vol., no., pp.1-7, 19-21 Sept. 2011

[51] Balke, R.L., "A Survey of Insulations for Aerospace Rotating Machines," in Aerospace, IEEE Transactions on , vol.1, no.2, pp.969-978, Aug. 1963

[52] Stranges, Meredith KW, Greg C. Stone, and Dennis L. Bogh. "New specs for ASD motors." Industry Applications Magazine, IEEE 13.1 (2007): 37-42.

[53] J. C. G. Wheeler, "Effects of Converter Pulses on the Electrical Insulation in Low and Medium Voltage Motors", IEEE Electrical Insulation Magazine, Vol.21, No.2, pp.22-29, 2005.

[54] R. Hebner, H. El-Kishky, M. Abdel-Salam, and F. Brown, "Higher Frequency Performance of Stress-Grading Systems for HV large Rotating Machines", IEEE Conference on Electrical Insulations and Dielectric Phenomena CEIDP 2006, pp. 218-221, 2006.

[55] J.C.G.Wheeler, A.M. Gully, A. E. Baker, and F. A. Perrot, "Thermal Performance of Stress Grading Systems for Converter-Fed Motors", IEEE Electrical Insulation Mag, Vol. 23, Issue 2, pp. 5-11, 2007.

[56] L. Ming E. et. al., "Effects of Repetitive Pulse Voltages on Surface Temperature increasing at End Corona Protection Region of High Voltage Motors", 10th INSUCON International Conference, Birmingham U.K., pp. 105-108, 2006.

[57] Kielmann and J Speck, "Behavior of the Stress Grading System in Converter Operated H.V. Machines", 10th INSUCON International Conference, Birmingham UK, pp. 99-104, 2006.

[58] Chen, William, and George Gao. "Using multi-stress aging test to evaluate and improve medium-voltage stator insulation for adjustable speed drive applications." Petroleum and Chemical Industry Conference (PCIC), 2011 Record of Conference Papers Industry Applications Society 58th Annual IEEE. IEEE, 2011.

[59] F. Espino-Cortes, S. Jayaram, and E. Cherney, "Stress Grading Materials for Cable Terminations under Fast Rise Time Pulses", IEEE Trans. on Dielectrics and Electrical Insulation, Vol.13, No.2, pp.430-435, 2006.

[60] Sharifi, E., S. Jayaram, and E.A. Cherney. A coupled electro-thermal study of the stress grading system of medium voltage motor coils when energized by repetitive fast pulses. in Electrical Insulation (ISEI), Conference Record of the 2010 IEEE International Symposium on. 2010.

[61] Koltunowicz, T.; Cavallini, A.; Djairam, D.; Montanari, G.C.; Smit, J., "The influence of square voltage waveforms on transformer insulation break down voltage," in Electrical Insulation and Dielectric Phenomena (CEIDP), 2011 Annual Report Conference on , vol., no., pp.48-51, 16-19 Oct. 2011

[62] Iván Arana Aristi, "Switching overvoltages in off-shore wind power grids. Measurements, modelling and validation in time and frequency domain", PhD Thesis, Technical University of Denmark, November 2011.

[63] Paulsson, L.; Ekehov, B.; Halen, S.; Larsson, T.; Palmqvist, L.; Edris, A.; Kidd, D.; Keri, A.J.F.; Mehraban, B., "High-frequency impacts in a converter-based back-to-back tie; the Eagle Pass installation," in Power Delivery, IEEE Transactions on , vol.18, no.4, pp.1410-1415, Oct. 2003

[64] Patel, U.; Jayaram, S.H.; El-Hag, A.; Seetahpathy, R.; , "MV cable termination failure assessment in the context of increased use of power electronics," Electrical Insulation Conference (EIC), 2011 , vol., no., pp.418-422, 5-8 June 2011

[65] Suzuki, H.; Mukai, S.; Ohki, Y.; Nakamichi, Y.; Ajiki, K., "Water-tree characteristics in low-density PE under simulated inverter voltages," IEEE Trans. on in Dielectrics and Electrical Insulation, vol.5, no.2, pp. 256-260, Apr 1998

[66] Suzuki, H., et al., Dielectric breakdown of low-density polyethylene under simulated inverter voltages. Dielectrics and Electrical Insulation, IEEE Transactions on, 1997. 4(2): p. 238-240.

[67] ASTM D 1676-03, Standard test methods for film-insulated magnet wire

[68] SANDIA Report 2013-7392, Humidity effects on wire insulation breakdown strength, 2013

[69] W. Yin, "Electric properties of an improved magnet wire for inverter-fed motors", IEEE Electrical Insulation Magazine, Vol.13, No.4, pp.17-23, 1997.

[70] H. Kikuchi, Y. Yukimori andS. Itonaga, "Inverter-surge resistant enameled wire based on nano-composite insulating material", Hitachi Cable Review, pp.55-62, 2002.

[71] M. Mesaki and H. Goda, "Hybrid composites of polyamid-imide and silica applied for wire insulation", Electrical Insulation Conference / Electrical Manufacturing &Coil Winding Expo 2001.

[72] F. R. Bohm, H. Schindler and K. Nagel, "Voltron TM - a new generation of wire enamel for the production of magnet wires for inverter fed motors", '02 INSUCON, pp.357-361, 2002.

[73] N. Hayakawa and H. Okubo, "Lifetime characteristics of nanocomposite enameld wire under surge voltage application", IEEE Electrical Insulation Magazine, Vol.24, pp.22-27, 2008.

[74] Kikuehi H (2004) Inverter Surge Resistance Enameled Wire Applied Nano-composite Insulating Material, The Papers of Teehnical Meeting on Dielectries and Electrieal Insulation, IEE Japan DEI-04-77:29-34 (in Japanese)

[75] Kikuehi H, Asano K (2006) Development of Organic/inorganic Nanocomposite Enameled Wire, IEEJ Trans. PE, 126-4:460-465 (in Japanese)

[76] Imai T, Sawa F, Ozaki T et al (2007) Expected Materials for the Future 7-7:6-13 (in Japanese)

[77] Ozaki T. Imai T, Sawa F et al (2005) Partial Diseharge Resistant Enameled Wire, Proceeding of Intemational Symposium on Electrical Insulating Materials (ISElM): 184-187